



**HAL**  
open science

## **Early Antiretroviral Therapy Preserves Functional Follicular Helper T and HIV-Specific B Cells in the Gut Mucosa of HIV-1-Infected Individuals**

Cyril Planchais, Laurent Hocqueloux, Clara Ibanez, Sébastien Gallien, Christiane Copie, Mathieu Surénaud, Ayrin Kök, Valerie Lorin, Mathieu Fusaro, Marie-Hélène Delfau-Larue, et al.

### ► To cite this version:

Cyril Planchais, Laurent Hocqueloux, Clara Ibanez, Sébastien Gallien, Christiane Copie, et al.. Early Antiretroviral Therapy Preserves Functional Follicular Helper T and HIV-Specific B Cells in the Gut Mucosa of HIV-1-Infected Individuals. *Journal of Immunology*, 2018, 200 (10), pp.3519-3529. 10.4049/jimmunol.1701615 . pasteur-02634634

**HAL Id: pasteur-02634634**

**<https://pasteur.hal.science/pasteur-02634634v1>**

Submitted on 10 Jun 2020

**HAL** is a multi-disciplinary open access archive for the deposit and dissemination of scientific research documents, whether they are published or not. The documents may come from teaching and research institutions in France or abroad, or from public or private research centers.

L'archive ouverte pluridisciplinaire **HAL**, est destinée au dépôt et à la diffusion de documents scientifiques de niveau recherche, publiés ou non, émanant des établissements d'enseignement et de recherche français ou étrangers, des laboratoires publics ou privés.

1 **Early antiretroviral therapy preserves functional follicular T Helper and HIV-specific**  
2 **B cells in the gut mucosa of HIV-1 infected individuals**

3

4 Cyril Planchais<sup>1,2</sup>, Laurent Hocqueloux<sup>3</sup>, Clara Ibanez<sup>1,2</sup>, Sébastien Gallien<sup>2,4</sup>, Christiane  
5 Copie<sup>5,6</sup>, Mathieu Surenaud<sup>1,2</sup>, Ayrin Kök<sup>7,8</sup>, Valérie Lorin<sup>7,8</sup>, Mathieu Fusaro<sup>11</sup>, Marie-  
6 Hélène Delfau-Larue<sup>11</sup>, Laurent Lefrou<sup>9</sup>, Thierry Prazuck<sup>3</sup>, Michael Lévy<sup>10</sup>, Nabila Seddiki<sup>1,2</sup>,  
7 Jean-Daniel Lelièvre<sup>1,2,4</sup>, Hugo Mouquet<sup>2,7,8</sup>, Yves Lévy<sup>1,2,4\*</sup>, Sophie Hüe<sup>1,2,11\*</sup>

8 <sup>1</sup>INSERM U955, Team 16, Université Paris Est Créteil, Faculté de Médecine, Créteil, F-  
9 94010, France

10 <sup>2</sup>Vaccine Research Institute (VRI), Université Paris Est Créteil, Faculté de Médecine, 94010,  
11 Créteil, France

12 <sup>3</sup>Service des Maladies Infectieuses et Tropicales, CHR d'Orléans-La Source, France

13 <sup>4</sup>Assistance Publique-Hôpitaux de Paris (AP-HP), Groupe Henri-Mondor Albert-Chenevier,  
14 Service d'immunologie clinique, Créteil, France

15 <sup>5</sup>Assistance Publique-Hôpitaux de Paris (AP-HP), Groupe Henri-Mondor Albert-Chenevier,  
16 Département de Pathologie, Créteil, France

17 <sup>6</sup>INSERM U955, Team 9, Université Paris Est Créteil, Faculté de Médecine, Créteil, F-94010,  
18 France

19 <sup>7</sup>Laboratory of Humoral Response to Pathogens, Department of Immunology, Institut Pasteur,

20 <sup>8</sup>INSERM U1222, Paris, 75015, France.

21 <sup>9</sup>Service d'Hépatogastro-entérologie, CHR d'Orléans-La Source, Orléans

22 <sup>10</sup>Assistance Publique-Hôpitaux de Paris (AP-HP), Groupe Henri-Mondor Albert-Chenevier,  
23 Service d'Hépatogastro-entérologie, Créteil, France

24 <sup>11</sup>Assistance Publique-Hôpitaux de Paris (AP-HP), Groupe Henri-Mondor Albert-Chenevier,  
25 Service d'immunologie biologique, Créteil, France

26 **\*Correspondence should be addressed to** Yves Lévy ([yves.levy@aphp.fr](mailto:yves.levy@aphp.fr)) and Sophie Hüe  
27 ([sophie.hue@aphp.fr](mailto:sophie.hue@aphp.fr)), CHU Henri Mondor, 94010 Créteil, FRANCE  
28 Phone: +33 149 812 298; Fax: +33 149 812 897.  
29 **Key words:** HIV, gut homeostasis, early antiretroviral therapy, B cells, T<sub>FH</sub> cells  
30 **Conflict of interest:** The authors have declared that no conflict of interest exists.  
31

32 ***ABSTRACT***

33 Human immunodeficiency virus-1 (HIV-1) infection is associated with B-cell dysregulation  
34 and dysfunction. In HIV-1-infected patients, we previously reported preservation of intestinal  
35 lymphoid structures and dendritic-cell maturation pathways after early combination  
36 antiretroviral therapy (e-ART), started during the acute phase of the infection, compared with  
37 late cART (l-ART) started during the chronic phase. Here, we investigated whether the timing  
38 of cART initiation was associated with the development of the HIV-1-specific humoral  
39 response in the gut. The results showed that e-ART was associated with higher frequencies of  
40 functional resting memory B cells in the gut. These frequencies correlated strongly with those  
41 of follicular helper T-cells ( $T_{FH}$ ) in the gut. Importantly, frequencies of HIV-1 Env gp140-  
42 reactive B cells were higher in patients given e-ART, in whom gp140-reactive IgG production  
43 by mucosal B cells increased after stimulation. Moreover, IL-21 release by peripheral-blood  
44 mononuclear cells stimulated with HIV-1 peptide pools was greater with e-ART than with L-  
45 ART. Thus, early treatment initiation helps to maintain HIV-1-reactive memory B cells in the  
46 gut, as well as  $T_{FH}$  cells, whose role is crucial in the development of potent affinity-matured  
47 and broadly neutralizing antibodies.

48 **INTRODUCTION**

49 Natural immunity to many viral diseases involves either circulating neutralizing  
50 antibodies produced by long-lived plasma cells in the bone marrow or the production of  
51 neutralizing antibodies by memory B cells reactivated by the infecting pathogen, frequently  
52 many years after the first exposure. For the HIV, however, the natural immune response  
53 appears ineffective (1). Among HIV-1-infected individuals, about 20% develop high titers of  
54 cross-reactive neutralizing antibodies to various regions of the HIV-1 envelope protein. In a  
55 few of these patients, known as elite neutralizers (about 1% of HIV-1-positive individuals),  
56 the cross-reactive antibodies include broadly neutralizing antibodies (bNAbs) capable of  
57 neutralizing most of the known HIV-1 strains (2). Unusual characteristics of bNAbs include  
58 high frequencies of V(D)J mutations, significantly extended third complementarity  
59 determining regions in the heavy-chain variable region (CDRH3), and polyreactivity and/or  
60 autoreactivity with human lipids and proteins (3).

61 The affinity-maturation process leading to the generation and selection of bNAb-  
62 expressing B cells remains poorly understood but must occur in germinal centers (GCs). Data  
63 from animal models demonstrate a critical role for follicular helper T-cells ( $T_{FH}$ ) in the  
64 induction of GCs needed for the development of a high-affinity, pathogen-specific antibody  
65 response (4). The  $T_{FH}$  cells are targeted by the HIV-1 very early after infection and constitute  
66 a major cellular compartment for HIV-1 replication and viral particle production in the lymph  
67 nodes of viremic individuals (5). Despite their high susceptibility to HIV-1 infection, many  
68 studies have shown abnormal  $T_{FH}$  cell accumulation in HIV-1-infected patients compared to  
69 uninfected individuals (6). Interestingly,  $T_{FH}$  cell frequencies correlate positively with plasma  
70 viremia levels, and  $T_{FH}$  cell accumulation diminishes with combination antiretroviral therapy  
71 (cART) (6). Circulating  $T_{FH}$  cells were recently identified as a memory compartment of  
72 tissue-resident  $T_{FH}$  cells and were shown to share with these an ability to produce IL-21 and

73 provide helper signals to B cells (7). Therefore, T<sub>FH</sub> function must be preserved to achieve  
74 efficient HIV-specific B-cell responses. T<sub>FH</sub> cells isolated from lymph nodes of HIV-1-  
75 infected individuals do not provide adequate B-cell help *in vitro* (8). One of the complex  
76 mechanisms involved in T<sub>FH</sub> cell dysfunction concerns the regulatory protein programmed  
77 death 1 (PD1). PD1 blockade has been shown to reinvigorate exhausted T cells (9).  
78 Incidentally, the PD1 ligand (PD-L1) has been described as highly expressed at the surface of  
79 B cells and dendritic cells in HIV-1-infected individuals (10, 11).

80 Previous studies have shown significant blood B-cell abnormalities in HIV-1-infected  
81 patients including an imbalance among peripheral mature B-cell subsets, with overexpression  
82 of tissue-like and activated memory B-cell subsets (12). HIV-associated exhaustion of tissue-  
83 like memory (TLM) B cells has been described based on a range of features and on  
84 similarities with T-cell exhaustion (13). These features include increased expression of  
85 multiple inhibitory receptors and weak proliferative and effector responses to various stimuli.  
86 Chronic immune activation appears to play a critical role in phenotypic and functional B-cell  
87 exhaustion. Conversely, resting memory (RM) B cells, which induce efficient secondary  
88 humoral responses, are depleted in the blood during the chronic stage of HIV-1 infection.  
89 When initiated at the chronic stage, cART fails to restore normal counts of blood memory B  
90 cells (14). In contrast, starting cART at the early stage of HIV-1 infection was associated with  
91 better restoration of RM B cells, in terms of both phenotype and function, as measured by the  
92 memory B-cell response to a recall antigen (15). Low RM B-cell counts may contribute to  
93 poor vaccine responses and weakened serological memory in HIV-1-infected individuals (16).

94 We previously reported that cART initiation during the early phase of HIV-1 infection  
95 (e-ART) ensured preservation of the mucosal gut lymphoid follicles (17). The tertiary  
96 lymphoid structures (TLSs) that develop during chronic inflammation can activate the  
97 molecular machinery needed to sustain *in situ* antibody diversification, isotype switching, B-

98 cell differentiation, and oligoclonal expansion, in keeping with their ability to function as  
99 active ectopic GCs. These observations raise the question of whether the timing of cART  
100 initiation may affect the development of the anti-HIV-1 humoral response in the gut. We  
101 designed a study to investigate this possibility.

102         The objective of this study was to compare e-ART to cART started later (l-ART),  
103 during the chronic stage of the infection, in terms of frequency, function, and specificity of  
104 mucosal T<sub>FH</sub> and B cells in the gut mucosa of HIV-1-infected individuals. We compared  
105 peripheral blood mononuclear cells (PBMCs) and rectal biopsies from patients identified  
106 retrospectively after several years of e-ART or l-ART. Frequencies of functional T<sub>FH</sub> and RM  
107 Env gp140-specific B cells in the gut mucosa were higher in the e-ART group. This finding  
108 supports a heretofore unsuspected role for the gut in generating antibodies against HIV-1.

109

110 **METHODS**

111 **Study participants**

112 Paired PBMCs and rectal biopsies were collected from 22 HIV-1-infected individuals  
113 who had been taking effective cART for several years. This treatment was started within 4  
114 months after the diagnosis of primary HIV-1 infection in 9 patients (early cART, e-ART  
115 group) and later on, i.e., during the chronic stage of HIV-1 infection (Fiebig stage VI) (18), in  
116 13 patients (late cART, l-ART group). The diagnosis of primary HIV-1 infection was defined  
117 as a negative or weakly positive ELISA with no more than four bands by Western blot and  
118 positive viremia and/or positive HIV-1 ELISA following a negative ELISA within the  
119 preceding 3 months. Gut biopsies from 6 HIV-1-seronegative individuals were included as  
120 controls. All rectal biopsies (~ 2 µm<sup>3</sup> each) were collected from the same site, 10-15 cm from  
121 the anal margin, to avoid potential bias due to regional variations among participants. **Table 1**  
122 reports the main features of the HIV-1-infected patients.

123

124 **Ethics statements**

125 All study participants provided written informed consent to participation in the study.  
126 This study was approved by our local ethics committee (Tours, France) (Comité de Protection  
127 des Personnes de Tours, 17<sup>th</sup> of December 2014, number: 2011-R26 (2011-CHRO-2011-02)

128

129 **HIV-1 envelope glycoproteins (HIV-1 Env gp)**

130 The recombinant HIV-1 Env YU-2 gp120 protein (gp120) and unlabeled HIV-1 and  
131 biotinylated YU-2 gp140 proteins (gp140 and gp140-biotin, respectively) were produced and  
132 purified as previously described (19, 20). Purified recombinant HIV-1 MN gp41 was provided  
133 by the NIH AIDS Reagent Program.

134

135 **Cell isolation from rectal biopsies**

136 Rectal biopsies were collected by rectoscopy at the regional hospital center in Orléans,  
137 France. Intraepithelial lymphocytes and lamina propria lymphocytes were obtained as  
138 previously described (17). Cells were used without further processing for  
139 immunophenotyping, ELISpot, and/or cell culture.

140

141 **PBMC stimulation and chemokine assays**

142 PBMCs ( $5 \cdot 10^5$ ) were incubated for 6 days at 37 °C in a final volume of 300 µL of  
143 complete RPMI medium (Gibco) supplemented with 10% human AB serum in 96 deep well  
144 plates (Greiner MasterBlock, Sigma-Aldrich), with or without stimulation by pools of 150  
145 HIV-1 15mer Gag or Env peptides (1 µg/mL, JPT, Berlin, Germany). *Staphylococcus aureus*  
146 enterotoxin B superantigen (SEB, 50 ng/mL) served as a positive control. Supernatants were  
147 collected after 6 days of culturing, aliquoted, and stored at -80 °C until use (21). IL-21 and  
148 IFN-γ produced in the supernatant by stimulated or unstimulated PBMCs were quantified  
149 using Luminex kits (ProcartaPlex, Affymetrix eBioscience, Thermo Fisher Scientific, San  
150 Diego, CA) according to the manufacturer's instructions. All samples were acquired on a  
151 Bioplex-200 instrument (Bio-Rad, Marnes-la-Coquette, France).

152

153 **Immunophenotype analysis**

154 The phenotypes of isolated mucosal B cells were assessed using FACS-staining with the  
155 following antibodies: anti-CD3-BV605 (SK7, BD Biosciences, Le Pont de Claix, France),  
156 anti-CD19-PECF594 (HIB19, BD Biosciences), anti-CD10-PECy7 (HI10a, Biolegend,  
157 Ozyme, Saint-Quentin en Yveline, France), anti-CD21-BV711 (B-Ly4, BD Biosciences),  
158 anti-CD27-APC (L128, BD Biosciences), anti-CD38-PerCP-Cy5.5 (HIT2, Biolegend,  
159 Ozyme), anti-IgG-BV421 (G18-145, BD Biosciences), and anti-IgA-FITC (IS11-8E10,

160 Miltenyi Biotec, Paris, France). Mucosal T<sub>FH</sub> cells were stained with antibodies to CD3-  
161 BV605 (SK7, BD Biosciences), CD4-PECF594 (RP4-T4, BD Biosciences), CXCR5-Alexa  
162 488 (RF8B2, BD Biosciences), and PD1-BV421 (EH12.EH7, Biolegend, Ozyme). For  
163 intracellular staining, cells were fixed and permeabilized using the FoxP3 staining buffer set  
164 (eBioscience, Thermo Fisher Scientific), washed, and incubated with anti-BCL6-PE (K112-  
165 91, BD Biosciences). For all cell stainings, dead cells were excluded from the gating by using  
166 the LIVE/DEAD fixable dead-cell stain kit (Molecular Probes, Invitrogen, Saint-Aubin,  
167 France). Cytometry acquisition was performed on an LSR II cytometer (BD Biosciences), and  
168 the data were analyzed using Flowjo software (Version 7.6.5; TreeStar, Ashland, OR).

169

#### 170 **B-cell clonality analyses**

171 DNA was extracted from frozen biopsies using the Qiasymphony automated extraction  
172 device (Qiagen, Hilden, Germany) according to the manufacturer's instructions. The B-cell  
173 repertoire was evaluated by detection of heavy-chain immunoglobulin (IgH) gene  
174 rearrangements according to BIOMED-2 guidelines (22). Briefly, three sets of VH primers  
175 corresponding to the three VH FR regions (FR1, FR2, and FR3) were used. Each set of  
176 primers consisted of six or seven oligonucleotides capable of annealing to their corresponding  
177 VH segments (VH1–VH7). These VH primer sets were used in conjunction with a single  
178 HEX-labeled JH consensus primer. After PCR, CDR3-derived products were loaded on a  
179 3130 Genetic Analyzer (Applied Biosystems, Foster City, CA) and fragment sizes were  
180 analyzed by GeneScan (Thermo Fisher Scientific).

181

#### 182 **In vitro B-cell differentiation into antibody-secreting cells (ASCs)**

183 Total cell-suspension isolated from rectal biopsies was incubated for 6 days in complete  
184 RPMI medium (Gibco) supplemented with 10% FCS, in 96-well plates (Nunc Maxisorp,

185 Roskilde, Denmark), alone or with immobilized LEAF purified agonist anti-CD40 antibody (5  
186  $\mu\text{g}/\text{mL}$ , Biolegend, Ozyme), recombinant human IL-4 (50 ng/ml, Cell Signaling, Ozyme), and  
187 IL-21 (50 ng/ml, Cell Signaling, Ozyme). Supernatants from 6-day-old cultures were  
188 collected and stored at  $-20^{\circ}\text{C}$ .

189

## 190 **ELISAs**

191 Polystyrene 96-well ELISA plates (Nunc Maxisorp) were coated with anti-human IgG  
192 ( $2.5 \mu\text{g}/\text{mL}$ , Jackson ImmunoResearch, Interchim, Montluçon, France) and anti-human IgA (5  
193  $\mu\text{g}/\text{mL}$ , HB200, (23)) in PBS overnight at  $4^{\circ}\text{C}$ . Plates were blocked by 2 hours' incubation  
194 with PBS containing 1% BSA (Sigma Aldrich). After washings, the plates were incubated for  
195 2 h with supernatants from cultures of differentiated B cells and 3-fold serial dilutions in PBS-  
196 1% BSA. The plates were then washed and incubated for 1 h with HRP-conjugated anti-  
197 human IgG, IgA, and IgM antibodies (Jackson ImmunoResearch, Interchim). Purified 10-1074  
198 monoclonal IgG (24) and IgA1 (23) antibodies ( $12 \mu\text{g}\cdot\text{mL}^{-1}$  starting concentration) were used  
199 as standards. To test HIV-1 gp140 reactivity, purified recombinant YU-2 gp140 trimers were  
200 coated ( $5 \mu\text{g}/\text{mL}$ ) on polystyrene 96-well ELISA plates (Nunc Maxisorp) overnight at  $4^{\circ}\text{C}$  in  
201 PBS. The plates were then blocked as described above and incubated for 2 h with IgGs  
202 secreted in B-cell culture supernatants, adjusted to a concentration of  $2 \mu\text{g}/\text{mL}$  in PBS-1%  
203 BSA. After washings, the plates were incubated for 1 h with HRP-conjugated anti-human IgG  
204 antibodies (Jackson ImmunoResearch, Interchim) then revealed using tetramethylbenzidine  
205 substrate (TMB, Life Technologies). Anti-HIV-1 gp140 monoclonal IgG antibodies 2F5 and  
206 2G12 (NIH AIDS Reagent Program) were used as positive controls.

207

## 208 **Immunohistochemistry**

209           Deparaffinized tissue sections were stained with mouse anti-human Pax-5 (DAK-*Pax5*,  
210   Dako Cytomation, Glostrup, Denmark) and rabbit anti-human PD-L1 (E1L3N, Cell Signaling,  
211   Ozyme) antibodies then with the anti-rabbit and anti-mouse IgG avidin–biotin complex  
212   system (ABC kit universal, Vectastain, Vector Laboratories, Les Ulis, France). Cell staining  
213   was performed using the DAB Substrate Kit for peroxidase (Vector Laboratories). All slides  
214   were counterstained with hematoxylin. Immunohistochemical images were acquired on a  
215   Zeiss Axioplan 2 (Göttingen, Germany) microscope equipped with an X20 (0.45 NA)  
216   objective, using a Zeiss Mrc digital camera (Göttingen, Germany) and AxioVision  
217   microscope software (Zeiss).

218

### 219   **Real-time quantitative PCR analysis**

220           Total RNAs were isolated from rectal biopsies using the RNeasy Micro Kit (Qiagen)  
221   according to the manufacturer’s protocol then retrotranscribed into cDNA molecules using the  
222   Affinity Script QPCR cDNA synthesis kit (Agilent, Santa Clara, CA). Quantitative PCRs  
223   were performed using the Brilliant II SYBR GREEN Q-PCR kit (Agilent) on the Mx3005  
224   QPCR Machine (Agilent). *OAZ-1* mRNA, whose expression was found to be stable across the  
225   three groups of participants, was used as a control for sample normalization. The relative  
226   levels of each gene were calculated using the  $2^{-\Delta\Delta CT}$  method.

227   The following primers were used (forward/reverse, 5’- 3’):

228   *OAZ-1*, ACTTATTCTACTCCGATGATCGAGAATCCTCGTCTTGTC (Invitrogen);

229   *IL-6*, CTCAGCCCTGAGAAAGGAGATTCTGCCAGTGCCTCTTTGC (Eurofins

230   Genomics, Les Ulis, France);

231   *IL-27p28* Ref Seq Accession no. NM\_145659.3 (Qiagen);

232   *EBI-3*, Ref Seq Accession no. NM\_005755.2 (Qiagen);

233   *AICDA*, Ref Seq Accession no. NM\_020661 (Qiagen);

234 *IL-12A*, AATGTTCCCATGCCTTCACCCAATCTCTTCAGAAGTGCAAGGG (Eurofins  
235 Genomics).

236

237 **Statistics**

238       Groups were compared using either the two-sided Mann-Whitney U test or the Kruskal-  
239 Wallis test. Spearman's rank test was applied to assess bivariate correlations and linear  
240 regression analysis performed to produce an accompanying best-fit line. All statistical  
241 analyses were performed using GraphPad Prism (version 6.0, GraphPad Software, La Jolla,  
242 CA).

243

244 **RESULTS**

245 ***Early treatment preserved mucosal resting memory B cells***

246 The phenotypes of cells freshly isolated from rectal biopsies were compared in HIV-1-  
247 infected patients given e-ART (n=7) or l-ART (n=8) and in HIV-negative controls (n=6).  
248 Table 1 reports the characteristics of the participants. Absolute counts of total CD19<sup>+</sup> B cells  
249 were significantly higher in the l-ART groups than in the control groups, with no difference  
250 between the e-ART and l-ART groups (**Figure 1a**). No differences were observed in term of  
251 CD19<sup>+</sup> B cells frequency between HIV1-infected groups and controls. By assessing  
252 differences in surface CD27 and CD21 expression in CD19<sup>+</sup> CD38<sup>low</sup> CD10<sup>-</sup> B cells, we  
253 identified mature naive (MN, CD27<sup>-</sup> CD21<sup>+</sup>), resting memory (RM, CD27<sup>+</sup> CD21<sup>+</sup>), tissue-  
254 like memory (TLM, CD27<sup>-</sup> CD21<sup>-</sup>), and activated memory (AM, CD27<sup>+</sup> CD21<sup>-</sup>) B cells  
255 (**Figure 1b**). As shown in **Figure 1c**, patients in both the cART groups exhibited lower  
256 frequencies of AM B cells (1.3%±0.5% and 1.6%±0.4%, respectively) compared to the  
257 controls (4.4%±1.5%) ( $P<0.001$  for both comparisons). Other B-cell subsets in e-ART  
258 patients were comparable to those from controls but differed significantly from those in l-  
259 ART patients, who had a lower frequency of RM B cells (39.6%±10.8% vs. 71.8%±15%,  
260  $P<0.001$ ) and higher frequencies of MN and TLM B cells (54.5%±11.6% and 2.6%±0.9% vs.  
261 23.3%±14.1% and 0.9%±0.6%,  $P<0.001$  and  $P<0.01$ , respectively). Blood B-cell phenotype  
262 was not substantially different between the e-ART and l-ART groups (**Supplemental Figure**  
263 **1**).

264

265 ***Mucosal antibody-secreting cells from late-treated patients displayed an immunoglobulin***  
266 ***profile skewed towards IgGs***

267 The frequencies of terminally differentiated B cells (antibody-secreting cells [ASCs],  
268 defined as CD19<sup>+</sup> CD27<sup>hi</sup> CD38<sup>+</sup> CD10<sup>-</sup>), known to be abundant in the gut mucosa (25), were

269 comparable in the e-ART and l-ART groups ( $38.5\% \pm 15.9\%$  vs.  $30.7\% \pm 13.3\%$ , respectively)  
270 (**Figure 2a**) but were significantly lower than in the control group ( $71.7\% \pm 12.3\%$ ,  $P < 0.001$   
271 for both comparisons). The total amount of immunoglobulins spontaneously released by  
272 freshly isolated mucosal ASCs cultured for 6 days was not different between the e-ART and l-  
273 ART groups (data not shown). In contrast, significant differences were noted regarding the  
274 immunoglobulin isotype profile. Thus, IgA release by ASCs from e-ART patients was greater  
275 compared to ASCs from l-ART patients ( $9.4 \pm 13.4 \mu\text{g/mL}$  vs.  $2.8 \pm 1.4 \mu\text{g/mL}$ ,  $P < 0.05$ ,  
276 respectively) and similar to that seen with ASCs from controls (**Figure 2b**). In contrast, the  
277 total amount of IgGs released by ASCs was significantly greater in the l-ART group than in  
278 the e-ART group ( $6.4 \pm 5.8 \mu\text{g/mL}$  vs.  $2.5 \pm 1.5 \mu\text{g/mL}$ ,  $P < 0.05$ ) (**Figure 2b**). The IgA/IgG ratio  
279 indicated skewing from IgAs to IgGs in the l-ART group compared to the e-ART group  
280 ( $0.68 \pm 0.72 \text{ AU}$  vs.  $9.4 \pm 15.24 \text{ AU}$ ,  $P < 0.001$ ) (data not shown). The IgA/IgG ratio differed  
281 significantly between the l-ART and control groups ( $0.68 \pm 0.72 \text{ AU}$  vs.  $2.89 \pm 1.93 \text{ AU}$ ,  
282  $P < 0.05$ ) but was comparable between the e-ART and control groups ( $9.4 \pm 15.24 \text{ AU}$  vs.  
283  $2.89 \pm 1.93 \text{ AU}$ ,  $P = 0.289$ ).

284 To evaluate whether the time of cART initiation might influence the mucosal B-cell  
285 repertoire in HIV-1-infected individuals, we studied B-cell clonality in the e-ART and l-ART  
286 groups (26). All patients in both groups displayed a normally distributed, polyclonal profile  
287 (**Figure 2c**) similar to that typically observed in healthy humans (27). Interestingly, some of  
288 the treated patients exhibited abnormal, preeminent, single peaks in their immunoglobulin  
289 spectratype (**Figure 2d**), suggesting clonal B-cell expansions in ectopic mucosal lymphoid  
290 structures such as those described in reactive lymphoproliferation (28, 29). Interestingly, these  
291 peaks were more common in the e-ART group than in the l-ART group, although the  
292 difference was not statistically significant ( $25\%$  vs.  $8.3\%$ ,  $P = 0.34$ ) (**Figure 2e**).

293

294 ***CD4<sup>+</sup> T follicular helper (T<sub>FH</sub>) cells are expanded in the mucosa of early-treated HIV-1-***  
295 ***infected patients***

296 The development of memory B cells within GC follicles depends heavily on the  
297 presence of T<sub>FH</sub> cells (30). The frequency of mucosal T<sub>FH</sub> cells, defined as  
298 CD3<sup>+</sup>CD4<sup>+</sup>PD1<sup>hi</sup>CXCR5<sup>+</sup>Bcl6<sup>+</sup> cells (**Figure 3a**), was significantly higher in the e-ART  
299 group than in the l-ART group (9.5%±5.1% vs. 1.6%±1.5% of CD3<sup>+</sup> CD4<sup>+</sup> cells,  $P<0.05$ ); the  
300 values in the e-ART and l-ART groups were significantly higher than in the controls  
301 (0.3%±0.3%,  $P<0.0001$  and  $P<0.05$ , respectively) (**Figure 3b**). As shown in **Figure 3c**, the  
302 frequency of T<sub>FH</sub> cells correlated significantly with the frequency of RM B cells ( $r=0.7542$ ,  
303  $P<0.01$ ). As illustrated in **Figure 3d**, an analysis of differential CXCR3 and CCR6 expression  
304 (31) allowed us to define three main circulating-T<sub>FH</sub> (c-T<sub>FH</sub>) cell subsets within blood CCR7<sup>-</sup>  
305 CXCR5<sup>+</sup>CD4<sup>+</sup>T cells: CXCR3<sup>+</sup>CCR6<sup>-</sup> (c-T<sub>FH</sub>1), CXCR3<sup>-</sup>CCR6<sup>-</sup> (c-T<sub>FH</sub>2), and  
306 CXCR3<sup>-</sup>CCR6<sup>+</sup> (c-T<sub>FH</sub>17). No differences in frequency or phenotype of c-T<sub>FH</sub> cells were  
307 observed between the e-ART and l-ART patients (**Figure 3e**).

308

309 ***Interaction between T<sub>FH</sub> cells and B cells in the gut of early-treated patients may promote***  
310 ***antibody generation***

311 The above-reported results and the role for PD-L1<sup>hi</sup> B cells in regulating T<sub>FH</sub>-cell  
312 expansion and function (8, 10) led us to investigate whether PD-L1 expression in mucosal  
313 follicles differed between the e-ART and l-ART groups. Single-cell expression of Pax5 and  
314 PD-L1 was sought by immunohistochemistry of rectal biopsies from e-ART (n=6) and l-ART  
315 (n=6) patients (**Figure 4a**). Based on Pax5 staining, B-cell follicle architecture differed  
316 between the two groups. All e-ART patients displayed well-defined secondary follicles,  
317 whereas most l-ART patients had some degree of B lymphoid area disorganization, with  
318 diffuse B-cell distribution in four of the six biopsies (patients g, h, j and m). PD-L1 expression

319 was clearly detectable in a single e-ART patient (patient e) and was not located in the B-cell  
320 area (**Figure 4a**). In contrast, PD-L1 expression was high in the follicles of five of the six  
321 biopsies from l-ART patients and was located within the B-cell area in three of these five  
322 biopsies (patients g, k, h) (**Figure 4b**).

323 Previous studies have established the importance of soluble factors such as IL-6 and  
324 IL-27 for the development and maintenance of T<sub>FH</sub> cells in mice and humans (32, 33). We  
325 used real-time quantitative polymerase chain reaction technology (RT-qPCR) to quantify the  
326 transcripts for IL-6 and the two IL-27 subunits (IL-27p28 and EBI3) in the rectal biopsies  
327 from patients in both HIV-1-positive groups (**Supplemental figure 2**). All three mRNAs  
328 were expressed at significantly higher levels in the e-ART group than the l-ART group (IL-6  
329 mRNA:  $4.39 \pm 6.14$  AU vs.  $0.76 \pm 0.57$  AU,  $P < 0.05$ ; IL-27p28 mRNA:  $0.12 \pm 0.22$  AU vs.  
330  $0.04 \pm 0.03$  AU,  $P < 0.05$ ; and EBI3 mRNA:  $0.21 \pm 0.09$  AU vs.  $0.08 \pm 0.04$  AU,  $P < 0.05$ ). The  
331 expression of control mRNAs encoding the IL-12A subunit, which also dimerize with EBI3 to  
332 form IL-35, was not different between the two HIV-positive groups ( $0.51 \pm 0.06$  AU vs.  
333  $0.49 \pm 0.15$  AU;  $P = 0.4127$ ). Crosstalk between B cells and T<sub>FH</sub> cells was investigated by RT-  
334 qPCR quantification of activation-induced cytidine deaminase (AID) transcripts. AID mRNA  
335 expression tended to be higher in mucosal GCs from e-ART patients compared to l-ART  
336 patients without reaching significance (**Supplemental Figure 2**,  $0.07 \pm 0.11$  AU vs.  
337  $0.006 \pm 0.007$  AU,  $P = 0.111$ ).

338

### 339 *Mucosal HIV-1 envelope-reactive memory B cells were expanded in early-treated HIV-1-* 340 *infected patients*

341 Next, we investigated whether HIV-1-specific B-cell responses were affected by the  
342 timing of cART initiation. We used flow cytometry to evaluate the frequency and phenotype  
343 of YU-2 gp140-reactive B cells. **Figure 5a** shows representative dot plots of CD19<sup>+</sup> gp140-

344 reactive cells from the patients and controls. Importantly, the frequency of mucosal gp140-  
345 reactive CD19<sup>+</sup> cells was significantly higher in the e-ART group than in the l-ART group  
346 (0.26%±0.09% vs. 0.07%±0.05%,  $P<0.01$ ) (**Figure 5b**) and the phenotype of these cells  
347 differed between the two groups (**Figure 5c**), with a predominance of RM cells in the e-ART  
348 group and a mixture of MN and RM cells in the l-ART group. Moreover, the frequency of  
349 mucosal gp140-reactive RM B cells was significantly higher in the e-ART group compared to  
350 the l-ART group (0.22%±0.14% vs. 0.05%±0.08%,  $P<0.05$ ) (**Figure 5c**). In line with these  
351 results, the frequency of gp140-reactive B cells expressing membrane-bound IgG was  
352 significantly higher in the e-ART group than in the l-ART group (0.28%±0.18% vs.  
353 0.06%±0.04%,  $P<0.05$ ) (**Figure 5d**). Finally, the frequency of total mucosal gp140-reactive B  
354 cells correlated significantly with that of T<sub>FH</sub> cells in the HIV-infected patients ( $r=0.7821$ ,  
355  $P<0.001$ ) (**Figure 5e**). We used an ELISA against trimeric YU-2 gp140 to test supernatants of  
356 freshly isolated mucosal B cells from both groups of HIV-1-infected patients, after 6 days of  
357 stimulation. In the e-ART group, compared to unstimulated mucosal B cells, stimulated cells  
358 released larger amounts of gp140-reactive IgGs (0 AU vs. 0.21±0.27 AU,  $P<0.01$ ) (**Figure**  
359 **5f**). Stimulation did not have this effect on cells from the l-ART group (**Figure 5f**).

360

361 *PBMCs from early-treated patients released larger amounts of IL-21 in response to*  
362 *stimulation with pools of HIV-1 peptides*

363 To further investigate the association between the time of cART initiation and the role  
364 for T<sub>FH</sub> cells in the development of HIV-1-specific B-cell responses, we evaluated IL-21  
365 production by PBMC. Indeed, IL-21 is primarily produced by CD4<sup>+</sup> T cells and is particularly  
366 critical to generation of antigen-specific IgG antibodies and expansion of class-switched B  
367 cells and plasma cells *in vivo*. Blood IL-21 secreting CD4<sup>+</sup> T cells share phenotypic and  
368 transcriptional similarities with lymphoid T<sub>FH</sub> cells in HIV-1-infected individuals (34). Given

369 the very limited number of total cells that can be retrieved from rectal biopsies, we used blood  
370 samples to quantify HIV-1-specific IL-21<sup>+</sup> and HIV-1-specific IFN- $\gamma$ <sup>+</sup> T cells in both HIV-1-  
371 positive groups. PBMCs stimulated with staphylococcal enterotoxin B (SEB) released  
372 significantly more IL-21 in the e-ART group than in the l-ART group (43.9 $\pm$ 35.9 pg/mL vs.  
373 10.9 $\pm$ 9.4 pg/mL  $P$ <0.01) (**Figure 6a, left panel**). Similarly, SEB-stimulated PBMCs released  
374 more IFN- $\gamma$  in the e-ART group than in the l-ART group (17 866.5 $\pm$ 9 512.6 pg/mL vs. 9  
375 186.4 $\pm$ 11 244.4 pg/mL,  $P$ <0.05) (**Figure 6a, right panel**). In addition, IL-21 release by  
376 PBMCs stimulated with pools of HIV-1 Env and Gag peptides was significantly more marked  
377 in the e-ART group (5.3 $\pm$ 3.5 pg/mL vs. 2.7 $\pm$ 2.9 pg/mL in the l-ART group,  $P$ <0.05) (**Figure**  
378 **6b**). In contrast, no statistically significant differences were observed between the e-ART and  
379 l-ART groups for the secretion of IFN- $\gamma$  by PBMCs stimulated with HIV-1 Env and Gag  
380 peptides (**Figure 6b**). In line with these results, the frequency of gp140-reactive B cells in  
381 blood was higher in the e-ART group (0.21% $\pm$ 0.12% vs. 0.1% $\pm$ 0.07%,  $P$ <0.05)  
382 (**Supplemental Figure 3**)

383

384

385 ***DISCUSSION***

386 Previous studies have shown that persistent infection with viruses such as the HIV-1  
387 lead to severe abnormalities in the dynamics of B-cell distribution and function in the blood  
388 and lymphoid organs, which very likely interfere with the establishment of an optimal  
389 antiviral humoral response (35). Far less is known about whether these alterations also occur  
390 in the gut mucosa and whether the timing of cART initiation influences B-cell phenotype and  
391 function. Our previous gene profiling study distinguished two groups of patients, based on  
392 pathway signatures of gut mucosal lymphoid structures and dendritic-cell function, which  
393 perfectly matched the timing of cART initiation (17). Here, we extend those data by  
394 demonstrating, at the cellular level, that early cART initiation preserves gut TLSs, which may  
395 function as active ectopic GCs characterized by high frequencies of functional T<sub>FH</sub> and  
396 gp140-reactive memory B cells. These GCs may play a critical role in the development of the  
397 antibody response.

398 In the gut, e-ART was associated with partial correction of the abnormal expansion of  
399 activated memory and TLM B cells and with preservation of RM B cells, conferring on e-  
400 ART patients a phenotype comparable to that of uninfected controls. In contrast, patients  
401 treated only at the chronic stage, despite experiencing long-term control of HIV replication,  
402 exhibited a profile suggesting impaired B-cell maturation, with a significant reduction in RM  
403 B cells. Finally, both groups of HIV-1-infected patients had similarly lower frequencies of  
404 ASCs compared to the uninfected control group. In contrast to findings at the mucosal levels,  
405 we did not find significant differences in the blood of early and late treated patients. These  
406 results differ from results reported by others (15, 36), and might be explained by a longer  
407 duration of ART treatment (more than 10 years on with an average of 4-21 years) in our  
408 cohort of l-ART patients. On the other hand, according to our results, a partial restoration of a  
409 normal homeostasis of B-cell populations with a decrease of activated memory and tissue-like

410 memory B cells has been reported in chronically ART treated patients (37, 38). Altogether,  
411 our results underscore the interest to study changes in B cell populations in various  
412 compartments revealing here that if e-ART may limit the major B-cell subset alterations in the  
413 gut, they are only partially restored even in the long term.

414         Although ASC frequencies in the gut were comparable in the e-ART and l-ART  
415 groups, the proportion of IgG-secreting cells was higher and the proportion of IgA-secreting  
416 cells commensurately lower in the l-ART group. The abnormal predominance of IgG in l-  
417 ART patients may reflect mucosal inflammation, which may contribute to impair gut mucosal  
418 homeostasis, as observed in inflammatory bowel disease (39). Moreover, the IgA secretion  
419 deficiency may cause changes in the composition of the intestinal microbiota (40) that may  
420 further activate the inflammatory processes seen in the gut of patients with chronic HIV-1  
421 infection despite effective cART (41). The skewing of IgA-secreting cells toward IgG-  
422 secreting cells is probably linked to microbial translocation and noninfectious complications  
423 associated with systemic inflammation. We therefore looked for abnormalities in global  
424 mucosal B-cell repertoires in the e-ART and l-ART groups, using the spectratyping method.  
425 Surprisingly, all HIV-1 infected patients displayed polyclonal profiles, although single  
426 expansions were noted, more often in the e-ART group than in the l-ART group. However,  
427 the global repertoire analyses by immunoglobulin spectratyping were performed on mucosal  
428 immunoglobulin-expressing and -secreting cells in the gut, including a high proportion of  
429 ASCs resulting from T-cell-independent differentiation of mucosal B cells. Given the massive  
430 T-cell depletion associated with HIV-1 infection (42), complete disorganization of ectopic  
431 mucosal GCs (17, 43), and crucial role for these GCs in memory B-cell development within  
432 TLSs (44), any disturbances in the B-cell repertoire would mainly concern the GC B cells (6)  
433 rather than the T-cell-independent ASCs.

434 In GCs, T<sub>FH</sub> cells are strongly involved in the development of memory B cells. Here, we  
435 found that T<sub>FH</sub> cells were expanded in the gut of HIV-1-infected patients compared to  
436 controls. Importantly, the frequency of gut T<sub>FH</sub> cells correlated with the frequency of RM B  
437 cells in the gut. These results are in line with previous reports showing T<sub>FH</sub> cell expansion in  
438 lymph node, spleen, and gut tissues of rhesus macaques infected with the SIV (45, 46) and in  
439 mucosal tissues from humanized-DRAG mouse models of HIV-1 infection (47). T<sub>FH</sub> cells  
440 decreased substantially with cART (6). Surprisingly, gut T<sub>FH</sub> remained significantly higher in  
441 the e-ART group than in the l-ART group whereas no differences were observed for cT<sub>FH</sub>  
442 frequency between the two groups. Our results underline the critical impact of tissue  
443 compartmentalization on T<sub>FH</sub> cell and B cells dynamics during HIV infection. In SIV infected  
444 rhesus macaques (RMs), T<sub>FH</sub> dynamics differs from one compartment to another (peripheral  
445 blood, vs LNs or spleen) (48). Indeed, microenvironment is essential for the differentiation  
446 and the maintenance of T<sub>FH</sub> cells. In the gut, the microbiota induces the differentiation of  
447 CD4<sup>+</sup> T cells into T<sub>FH</sub> cells, thereby promoting the secretion of microbial-specific IgAs,  
448 which are important for controlling the microflora and maintaining gut homeostasis (49).  
449 Thus, T<sub>FH</sub> expansion in HIV-1-infected patients may be seen as a mechanism that  
450 compensates for the massive Th17 depletion, thereby helping to maintain gut homeostasis.  
451 This hypothesis is supported by studies in ROR $\gamma$ t-deficient mice, in which large numbers of  
452 TLSs are required to contain the microbiota (50).

453  $T_{FH}$  dynamics varies according to the severity of the disease. Slow progressor RMs display an  
454 increased frequency of  $T_{FH}$  cells in LNs whereas their numbers drastically decreased in fast  
455 progressors RMs (51, 52). Evidences support the pivotal role of persistent viral antigen within  
456 the GC in driving  $T_{FH}$  cell expansion and the disruption of GC organization coincides with the  
457 loss of  $T_{FH}$  cells and the onset of AIDS in terminal stages of HIV infection (51). CXCL13 has  
458 been described to be a plasma biomarker of germinal center activity in HIV-infected humans  
459 (53). In our cohort of 56 l-ART patients and 17 e-ART patients, CXCL13 tended to be higher  
460 in the sera of e-ART patients compared to l-ART patients without reaching significance (data  
461 not shown). We have previously reported a loss of FDC network and TLS in the gut of l-ART  
462 patients. Thus, this may impact  $T_{FH}$  maintenance in l-ART patients.

463 The difference of  $T_{FH}$  frequencies between e-ART and l-ART patients may also reflect  
464 distinct immune response of  $T_{FH}$  cells depending on the nature of help signals, consisting of  
465 both cytokines and cell surface molecules. We therefore investigated the signaling factors that  
466 contribute to  $T_{FH}$  expansion. Studies in SIV-infection models (46) and in mice (33)  
467 established a key role for IL-6 and IL-27 signaling in  $T_{FH}$  cell function and GC responses. In  
468 our study, IL-6 and IL-27 transcript levels in the gut were higher with e-ART than with l-ART.  
469 In addition to signaling mediators, B-cell dysregulation may also be involved in the reduced  
470 frequency and impaired function of  $T_{FH}$  cells in HIV-1 infection (8). PD-L1 expression on B  
471 cells and PD-1 receptor engagement on  $T_{FH}$  cells decrease IL-21 secretion and cell  
472 proliferation (8, 10). We found that the proportion of TLS B cells expressing PD-L1 was  
473 greater in the l-ART group than in the e-ART group. These results suggest that e-ART  
474 patients had functional  $T_{FH}$  cells capable of contributing to the development of antigen-  
475 specific B-cell responses in gut GCs.

476

477           Recent work highlighted the importance of maintaining functional GCs for the  
478 development of HIV-1 bNAbs (54). We therefore hypothesized that functional HIV-1-specific  
479 T<sub>FH</sub> cells enhanced HIV-1-specific B-cell responses in the gut. In keeping with this  
480 hypothesis, the frequencies of T<sub>FH</sub> and gp140-reactive memory B cells in gut TLSs were  
481 higher in the e-ART group than in the l-ART group. Interestingly, the frequency of gut T<sub>FH</sub>  
482 cells correlated with the frequency of gut gp140-reactive memory B cells in cART-treated  
483 HIV-1-infected patients. In line with these results, it has been recently shown that HIV Env-  
484 specific CXCR5<sup>+</sup> CD4<sup>+</sup> T cells that secrete interleukin-21 are strongly associated with B cell  
485 memory phenotypes and function (55). The results suggested that circulating total and HIV-1-  
486 specific IL-21-producing T cells were more abundant with e-ART than with l-ART. In  
487 contrast, counts of circulating IFN- $\gamma$ -secreting HIV-1-specific T cells were not significantly  
488 different between the two groups. It is tempting to speculate that the HIV-1 specificity of gut  
489 T<sub>FH</sub> cells may be extrapolated from the amount of IL-21 released by T cells in response to  
490 stimulation with a pool of HIV-1 peptides. Thus, TLSs may act as active ectopic GCs and  
491 may play a critical role in the development of the affinity-matured HIV-1-specific antibody  
492 response.

493           The first HIV-1-reactive antibodies become detectable about 13 days after HIV-1  
494 transmission (56) and are mainly directed against the Env gp41, in both blood and the  
495 terminal ileum. Most of these gp41 antibodies are polyreactive affinity-matured IgGs that  
496 target self- and microbial antigens (57). Using an *in vitro* B-cell-to-ASC differentiation assay,  
497 we confirmed that the frequency of gp140-reactive memory B cells was higher with e-ART  
498 than with l-ART, as shown by the larger amount of anti-gp140 reactive IgGs detectable by  
499 ELISA in the e-ART group. The anti-gp140 IgGs targeted the gp41 portion of the HIV-1 Env  
500 protein (data not shown). Mucosal B-cell clones can re-enter a germinal center, where they  
501 undergo further somatic hypermutation to produce high-affinity IgA that is adapted to the

502 changing composition of the microbiota. It is tempting to speculate that gp140-reactive  
503 memory B cells may be a good target for therapeutic vaccine. Indeed, a recent study of the  
504 pre-vaccination B-cell repertoire identified a preexisting pool of microbiome-gp41 cross-  
505 reactive B cells that was stimulated by the vaccine (58). Extensive molecular characterization  
506 of the gp-140-reactive B cells would be important to explore the potential beneficial effects of  
507 e-ART on the development of a potent HIV-1-specific humoral immune response in the gut.

508         The beneficial impact of e-ART on the circulating B-cell populations is now well-  
509 documented (15). Here, we demonstrated that e-ART may also lessen the alterations in  
510 mucosal B-cell subsets. The protection afforded by a potent mucosal humoral response is  
511 particularly important in the gut, where the intestinal barrier is continuously attacked by the  
512 microbiota. GC preservation may contribute to diversification of the mucosal B-cell  
513 repertoire, thereby helping to control the billions of microorganisms found in the gut lumen  
514 (59). Thus, e-ART may contribute to reduce the appearance of non-HIV-1 AIDS-related  
515 gastrointestinal syndromes. Considerable effort is being put into creating a vaccine-based  
516 strategy for developing HIV-1 bNAbs in infected patients. A common feature of bNAbs is a  
517 higher level of somatic hypermutations compared to that seen in typical immune responses  
518 (60, 61), which is generated after multiple cell passages through GCs containing target  
519 antigens. We demonstrated that e-ART helped to preserve intestinal GC functions and was  
520 associated with a higher frequency of HIV-1 Env gp140-specific B cells in the gut compared  
521 to l-ART. This finding suggests that eliciting potent anti-HIV-1 antibodies at mucosal sites  
522 may require e-ART, to maintain an optimal mucosal GC response by preserving T<sub>FH</sub> cells  
523 function and, therefore, maturing GC B cells.

524

525

526

527 **Acknowledgments**

528 The HIV-1 Env gp41 (0671) was obtained from the center for AIDS Reagents, NIBSC, UK  
529 supported by EURIPRED (EC FP7 INFRASTRUCTURES-2012-INFRA-2012-1.1.5.: Grant  
530 Number 31266). This work was supported by the SIDACTION foundation, the ANRS and the  
531 Labex Vaccine Research Institute (VRI) (Investissements d'Avenir program managed by the  
532 ANR under reference ANR-10-LABX-77-01).

533

534 **Author contributions**

535 SH and YL conceived and supervised the study.

536 SH, YL, HM, and CP designed the experiments and analyzed the data.

537 CP, CI, MS, CC, MF, and MHDL performed the experiments.

538 LH, SG, LL, TP, and ML recruited the participants and collected the samples.

539 SH, YL, HM, and CP wrote the manuscript, with contributions from all authors.

540

541

542 **References**

- 543 1. Tomaras, G. D., and B. F. Haynes. 2009. HIV-1-specific antibody responses during acute and  
544 chronic HIV-1 infection. *Current opinion in HIV and AIDS* 4: 373-379.
- 545 2. Mouquet, H. 2014. Antibody B cell responses in HIV-1 infection. *Trends in immunology* 35:  
546 549-561.
- 547 3. Kelsoe, G., and B. F. Haynes. 2017. Host controls of HIV broadly neutralizing antibody  
548 development. *Immunological reviews* 275: 79-88.
- 549 4. Crotty, S. 2014. T follicular helper cell differentiation, function, and roles in disease. *Immunity*  
550 41: 529-542.
- 551 5. Perreau, M., A. L. Savoye, E. De Crignis, J. M. Corpataux, R. Cubas, E. K. Haddad, L. De Leval,  
552 C. Graziosi, and G. Pantaleo. 2013. Follicular helper T cells serve as the major CD4 T cell  
553 compartment for HIV-1 infection, replication, and production. *The Journal of experimental*  
554 *medicine* 210: 143-156.
- 555 6. Lindqvist, M., J. van Lunzen, D. Z. Soghoian, B. D. Kuhl, S. Ranasinghe, G. Kranias, M. D.  
556 Flanders, S. Cutler, N. Yudanin, M. I. Muller, I. Davis, D. Farber, P. Hartjen, F. Haag, G. Alter, J.  
557 Schulze zur Wiesch, and H. Streeck. 2012. Expansion of HIV-specific T follicular helper cells in  
558 chronic HIV infection. *The Journal of clinical investigation* 122: 3271-3280.
- 559 7. Locci, M., C. Havenar-Daughton, E. Landais, J. Wu, M. A. Kroenke, C. L. Arlehamn, L. F. Su, R.  
560 Cubas, M. M. Davis, A. Sette, E. K. Haddad, A. V. I. P. C. P. I. International, P. Pognard, and S.  
561 Crotty. 2013. Human circulating PD-1+CXCR3-CXCR5+ memory Tfh cells are highly functional  
562 and correlate with broadly neutralizing HIV antibody responses. *Immunity* 39: 758-769.
- 563 8. Cubas, R. A., J. C. Mudd, A. L. Savoye, M. Perreau, J. van Grevenynghe, T. Metcalf, E. Connick,  
564 A. Meditz, G. J. Freeman, G. Abesada-Terk, Jr., J. M. Jacobson, A. D. Brooks, S. Crotty, J. D.  
565 Estes, G. Pantaleo, M. M. Lederman, and E. K. Haddad. 2013. Inadequate T follicular cell help  
566 impairs B cell immunity during HIV infection. *Nature medicine* 19: 494-499.
- 567 9. Finnefrock, A. C., A. Tang, F. Li, D. C. Freed, M. Feng, K. S. Cox, K. J. Sykes, J. P. Guare, M. D.  
568 Miller, D. B. Olsen, D. J. Hazuda, J. W. Shiver, D. R. Casimiro, and T. M. Fu. 2009. PD-1  
569 blockade in rhesus macaques: impact on chronic infection and prophylactic vaccination. *J*  
570 *Immunol* 182: 980-987.
- 571 10. Khan, A. R., E. Hams, A. Floudas, T. Sparwasser, C. T. Weaver, and P. G. Fallon. 2015. PD-L1hi  
572 B cells are critical regulators of humoral immunity. *Nature communications* 6: 5997.
- 573 11. Planes, R., L. BenMohamed, K. Leghmari, P. Delobel, J. Izopet, and E. Bahraoui. 2014. HIV-1  
574 Tat protein induces PD-L1 (B7-H1) expression on dendritic cells through tumor necrosis factor  
575 alpha- and toll-like receptor 4-mediated mechanisms. *J Virol* 88: 6672-6689.
- 576 12. Moir, S., and S. F. Anthony. 2013. Insights into B cells and HIV-specific B-cell responses in HIV-  
577 infected individuals. *Immunological Reviews* 254.
- 578 13. Moir, S., J. Ho, A. Malaspina, W. Wang, A. C. DiPoto, M. A. O'Shea, G. Roby, S. Kottlilil, J.  
579 Arthos, M. A. Proschan, T. W. Chun, and A. S. Fauci. 2008. Evidence for HIV-associated B cell  
580 exhaustion in a dysfunctional memory B cell compartment in HIV-infected viremic  
581 individuals. *The Journal of experimental medicine* 205: 1797-1805.
- 582 14. Pensiero, S., L. Galli, S. Nozza, N. Ruffin, A. Castagna, G. Tambussi, B. Hejdeman, D.  
583 Misciagna, A. Riva, M. Malnati, F. Chiodi, and G. Scarlatti. 2013. B-cell subset alterations and  
584 correlated factors in HIV-1 infection. *Aids* 27: 1209-1217.
- 585 15. Moir, S., C. M. Buckner, J. Ho, W. Wang, J. Chen, A. J. Waldner, J. G. Posada, L. Kardava, M. A.  
586 O'Shea, S. Kottlilil, T. W. Chun, M. A. Proschan, and A. S. Fauci. 2010. B cells in early and  
587 chronic HIV infection: evidence for preservation of immune function associated with early  
588 initiation of antiretroviral therapy. *Blood* 116: 5571-5579.
- 589 16. Cagigi, A., A. Nilsson, S. Pensiero, and F. Chiodi. 2010. Dysfunctional B-cell responses  
590 during HIV-1 infection: implication for influenza vaccination and highly active antiretroviral  
591 therapy. *The Lancet. Infectious diseases* 10: 499-503.

- 592 17. Kok, A., L. Hocqueloux, H. Hocini, M. Carriere, L. Lefrou, A. Guguin, P. Tisserand, H.  
593 Bonnabau, V. Avettand-Fenoel, T. Prazuck, S. Katsahian, P. Gaulard, R. Thiebaut, Y. Levy, and  
594 S. Hue. 2015. Early initiation of combined antiretroviral therapy preserves immune function  
595 in the gut of HIV-infected patients. *Mucosal immunology* 8: 127-140.
- 596 18. Fiebig, E. W., D. J. Wright, B. D. Rawal, P. E. Garrett, R. T. Schumacher, L. Peddada, C.  
597 Heldebrant, R. Smith, A. Conrad, S. H. Kleinman, and M. P. Busch. 2003. Dynamics of HIV  
598 viremia and antibody seroconversion in plasma donors: implications for diagnosis and staging  
599 of primary HIV infection. *AIDS* 17: 1871-1879.
- 600 19. Mouquet, H., F. Klein, J. F. Scheid, M. Warncke, J. Pietzsch, T. Y. Oliveira, K. Velinzon, M. S.  
601 Seaman, and M. C. Nussenzweig. 2011. Memory B cell antibodies to HIV-1 gp140 cloned from  
602 individuals infected with clade A and B viruses. *PLoS one* 6: e24078.
- 603 20. Mouquet, H., L. Scharf, Z. Euler, Y. Liu, C. Eden, J. F. Scheid, A. Halper-Stromberg, P. N.  
604 Gnanapragasam, D. I. Spencer, M. S. Seaman, H. Schuitemaker, T. Feizi, M. C. Nussenzweig,  
605 and P. J. Bjorkman. 2012. Complex-type N-glycan recognition by potent broadly neutralizing  
606 HIV antibodies. *Proceedings of the National Academy of Sciences of the United States of*  
607 *America* 109: E3268-3277.
- 608 21. Surenaud, M., C. Manier, L. Richert, R. Thiebaut, Y. Levy, S. Hue, and C. Lacabaratz. 2016.  
609 Optimization and evaluation of Luminex performance with supernatants of antigen-  
610 stimulated peripheral blood mononuclear cells. *BMC immunology* 17: 44.
- 611 22. McDonald, T. J., L. Kuo, and F. C. Kuo. 2017. Determination of VH Family Usage in B-Cell  
612 Malignancies via the BIOMED-2 IGH PCR Clonality Assay. *American journal of clinical*  
613 *pathology* 147: 549-556.
- 614 23. Lorin, V., and H. Mouquet. 2015. Efficient generation of human IgA monoclonal antibodies.  
615 *Journal of immunological methods* 422: 102-110.
- 616 24. Malbec, M., F. Porrot, R. Rua, J. Horwitz, F. Klein, A. Halper-Stromberg, J. F. Scheid, C. Eden,  
617 H. Mouquet, M. C. Nussenzweig, and O. Schwartz. 2013. Broadly neutralizing antibodies that  
618 inhibit HIV-1 cell to cell transmission. *The Journal of experimental medicine* 210: 2813-2821.
- 619 25. Landsverk, O. J., O. Snir, R. B. Casado, L. Richter, J. E. Mold, P. Reu, R. Horneland, V. Paulsen,  
620 S. Yaqub, E. M. Aandahl, O. M. Oyen, H. S. Thorarensen, M. Salehpour, G. Possnert, J. Frisen,  
621 L. M. Sollid, E. S. Baekkevold, and F. L. Jahnsen. 2017. Antibody-secreting plasma cells persist  
622 for decades in human intestine. *The Journal of experimental medicine* 214: 309-317.
- 623 26. Guzman, L. M., D. Castillo, and S. O. Aguilera. 2010. Polymerase chain reaction (PCR)  
624 detection of B cell clonality in Sjogren's syndrome patients: a diagnostic tool of clonal  
625 expansion. *Clinical and experimental immunology* 161: 57-64.
- 626 27. Dong, L., Y. Masaki, T. Takegami, Z. X. Jin, C. R. Huang, T. Fukushima, T. Sawaki, T. Kawanami,  
627 T. Saeki, K. Kitagawa, S. Sugai, T. Okazaki, Y. Hirose, and H. Umehara. 2007. Clonality analysis  
628 of lymphoproliferative disorders in patients with Sjogren's syndrome. *Clinical and*  
629 *experimental immunology* 150: 279-284.
- 630 28. Langerak, A. W., T. J. Molina, F. L. Lavender, D. Pearson, T. Flohr, C. Sambade, E. Schuurin, T.  
631 Al Saati, J. J. van Dongen, and J. H. van Krieken. 2007. Polymerase chain reaction-based  
632 clonality testing in tissue samples with reactive lymphoproliferations: usefulness and pitfalls.  
633 A report of the BIOMED-2 Concerted Action BMH4-CT98-3936. *Leukemia* 21: 222-229.
- 634 29. Evans, P. A., C. Pott, P. J. Groenen, G. Salles, F. Davi, F. Berger, J. F. Garcia, J. H. van Krieken, S.  
635 Pals, P. Kluin, E. Schuurin, M. Spaargaren, E. Boone, D. Gonzalez, B. Martinez, R. Villuendas,  
636 P. Gameiro, T. C. Diss, K. Mills, G. J. Morgan, G. I. Carter, B. J. Milner, D. Pearson, M. Hummel,  
637 W. Jung, M. Ott, D. Canioni, K. Beldjord, C. Bastard, M. H. Delfau-Larue, J. J. van Dongen, T. J.  
638 Molina, and J. Cabecadas. 2007. Significantly improved PCR-based clonality testing in B-cell  
639 malignancies by use of multiple immunoglobulin gene targets. Report of the BIOMED-2  
640 Concerted Action BHM4-CT98-3936. *Leukemia* 21: 207-214.
- 641 30. Rankin, A. L., H. MacLeod, S. Keegan, T. Andreyeva, L. Lowe, L. Bloom, M. Collins, C.  
642 Nickerson-Nutter, D. Young, and H. Guay. 2011. IL-21 receptor is critical for the development  
643 of memory B cell responses. *Journal of immunology* 186: 667-674.

- 644 31. Morita, R., N. Schmitt, S. E. Bentebibel, R. Ranganathan, L. Bourdery, G. Zurawski, E. Foucat,  
645 M. Dullaers, S. Oh, N. Sabzghabaei, E. M. Lavecchio, M. Punaro, V. Pascual, J. Banchereau,  
646 and H. Ueno. 2011. Human blood CXCR5(+)CD4(+) T cells are counterparts of T follicular cells  
647 and contain specific subsets that differentially support antibody secretion. *Immunity* 34: 108-  
648 121.
- 649 32. Nurieva, R. I., Y. Chung, D. Hwang, X. O. Yang, H. S. Kang, L. Ma, Y. H. Wang, S. S. Watowich,  
650 A. M. Jetten, Q. Tian, and C. Dong. 2008. Generation of T follicular helper cells is mediated by  
651 interleukin-21 but independent of T helper 1, 2, or 17 cell lineages. *Immunity* 29: 138-149.
- 652 33. Batten, M., N. Ramamoorthi, N. M. Kljavin, C. S. Ma, J. H. Cox, H. S. Dengler, D. M. Danilenko,  
653 P. Caplazi, M. Wong, D. A. Fulcher, M. C. Cook, C. King, S. G. Tangye, F. J. de Sauvage, and N.  
654 Ghilardi. 2010. IL-27 supports germinal center function by enhancing IL-21 production and  
655 the function of T follicular helper cells. *The Journal of experimental medicine* 207: 2895-2906.
- 656 34. Schultz, B. T., J. E. Teigler, F. Pissani, A. F. Oster, G. Kranias, G. Alter, M. Marovich, M. A. Eller,  
657 U. Dittmer, M. L. Robb, J. H. Kim, N. L. Michael, D. Bolton, and H. Streeck. 2016. Circulating  
658 HIV-Specific Interleukin-21(+)CD4(+) T Cells Represent Peripheral Tfh Cells with Antigen-  
659 Dependent Helper Functions. *Immunity* 44: 167-178.
- 660 35. Moir, S., and A. S. Fauci. 2009. B cells in HIV infection and disease. *Nature reviews.*  
661 *Immunology* 9: 235-245.
- 662 36. van Grevenynghe, J., R. A. Cubas, A. Noto, S. DaFonseca, Z. He, Y. Peretz, A. Filali-Mouhim, F.  
663 P. Dupuy, F. A. Procopio, N. Chomont, R. S. Balderas, E. A. Said, M. R. Boulassel, C. L.  
664 Tremblay, J. P. Routy, R. P. Sekaly, and E. K. Haddad. 2011. Loss of memory B cells during  
665 chronic HIV infection is driven by Foxo3a- and TRAIL-mediated apoptosis. *The Journal of*  
666 *clinical investigation* 121: 3877-3888.
- 667 37. Luo, Z., L. Ma, L. Zhang, L. Martin, Z. Wan, S. Warth, A. Kilby, Y. Gao, P. Bhargava, Z. Li, H. Wu,  
668 E. G. Meissner, Z. Li, J. M. Kilby, G. Liao, and W. Jiang. 2016. Key differences in B cell  
669 activation patterns and immune correlates among treated HIV-infected patients versus  
670 healthy controls following influenza vaccination. *Vaccine* 34: 1945-1955.
- 671 38. Pogliaghi, M., M. Ripa, S. Pensiero, M. Tolazzi, S. Chiappetta, S. Nozza, A. Lazzarin, G.  
672 Tambussi, and G. Scarlatti. 2015. Beneficial Effects of cART Initiated during Primary and  
673 Chronic HIV-1 Infection on Immunoglobulin-Expression of Memory B-Cell Subsets. *PloS one*  
674 10: e0140435.
- 675 39. Gutzeit, C., G. Magri, and A. Cerutti. 2014. Intestinal IgA production and its role in host-  
676 microbe interaction. *Immunological reviews* 260: 76-85.
- 677 40. Peterson, D. A., N. P. McNulty, J. L. Guruge, and J. I. Gordon. 2007. IgA response to symbiotic  
678 bacteria as a mediator of gut homeostasis. *Cell host & microbe* 2: 328-339.
- 679 41. Somsouk, M., J. D. Estes, C. Deleage, R. M. Dunham, R. Albright, J. M. Inadomi, J. N. Martin, S.  
680 G. Deeks, J. M. McCune, and P. W. Hunt. 2015. Gut epithelial barrier and systemic  
681 inflammation during chronic HIV infection. *Aids* 29: 43-51.
- 682 42. Clayton, F., G. Snow, S. Reka, and D. P. Kotler. 1997. Selective depletion of rectal lamina  
683 propria rather than lymphoid aggregate CD4 lymphocytes in HIV infection. *Clinical and*  
684 *experimental immunology* 107: 288-292.
- 685 43. Zhang, Z. Q., D. R. Casimiro, W. A. Schleif, M. Chen, M. Citron, M. E. Davies, J. Burns, X. Liang,  
686 T. M. Fu, L. Handt, E. A. Emini, and J. W. Shiver. 2007. Early depletion of proliferating B cells  
687 of germinal center in rapidly progressive simian immunodeficiency virus infection. *Virology*  
688 361: 455-464.
- 689 44. Lindner, C., I. Thomsen, B. Wahl, M. Ugur, M. K. Sethi, M. Friedrichsen, A. Smoczek, S. Ott, U.  
690 Baumann, S. Suerbaum, S. Schreiber, A. Bleich, V. Gaboriau-Routhiau, N. Cerf-Bensussan, H.  
691 Hazanov, R. Mehr, P. Boysen, P. Rosenstiel, and O. Pabst. 2015. Diversification of memory B  
692 cells drives the continuous adaptation of secretory antibodies to gut microbiota. *Nature*  
693 *immunology* 16: 880-888.
- 694 45. Hong, J. J., P. K. Amancha, K. Rogers, A. A. Ansari, and F. Villinger. 2012. Spatial alterations  
695 between CD4(+) T follicular helper, B, and CD8(+) T cells during simian immunodeficiency

- 696 virus infection: T/B cell homeostasis, activation, and potential mechanism for viral escape.  
697 *Journal of immunology* 188: 3247-3256.
- 698 46. Petrovas, C., T. Yamamoto, M. Y. Gerner, K. L. Boswell, K. Wloka, E. C. Smith, D. R. Ambrozak,  
699 N. G. Sandler, K. J. Timmer, X. Sun, L. Pan, A. Poholek, S. S. Rao, J. M. Brenchley, S. M. Alam,  
700 G. D. Tomaras, M. Roederer, D. C. Douek, R. A. Seder, R. N. Germain, E. K. Haddad, and R. A.  
701 Koup. 2012. CD4 T follicular helper cell dynamics during SIV infection. *The Journal of clinical*  
702 *investigation* 122: 3281-3294.
- 703 47. Allam, A., S. Majji, K. Peachman, L. Jagodzinski, J. Kim, S. Ratto-Kim, W. Wijayalath, M.  
704 Merbah, J. H. Kim, N. L. Michael, C. R. Alving, S. Casares, and M. Rao. 2015. TFH cells  
705 accumulate in mucosal tissues of humanized-DRAG mice and are highly permissive to HIV-1.  
706 *Scientific reports* 5: 10443.
- 707 48. Moukambi, F., H. Rabezanahary, V. Rodrigues, G. Racine, L. Robitaille, B. Krust, G. Andreani,  
708 C. Soundaramourty, R. Silvestre, M. Laforge, and J. Estaquier. 2015. Early Loss of Splenic Tfh  
709 Cells in SIV-Infected Rhesus Macaques. *PLoS pathogens* 11: e1005287.
- 710 49. Kubinak, J. L., C. Petersen, W. Z. Stephens, R. Soto, E. Bake, R. M. O'Connell, and J. L. Round.  
711 2015. MyD88 signaling in T cells directs IgA-mediated control of the microbiota to promote  
712 health. *Cell host & microbe* 17: 153-163.
- 713 50. Lochner, M., C. Ohnmacht, L. Presley, P. Bruhns, M. Si-Tahar, S. Sawa, and G. Eberl. 2011.  
714 Microbiota-induced tertiary lymphoid tissues aggravate inflammatory disease in the absence  
715 of RORgamma t and LTi cells. *The Journal of experimental medicine* 208: 125-134.
- 716 51. Xu, H., X. Wang, N. Malam, A. A. Lackner, and R. S. Veazey. 2015. Persistent Simian  
717 Immunodeficiency Virus Infection Causes Ultimate Depletion of Follicular Th Cells in AIDS.  
718 *Journal of immunology* 195: 4351-4357.
- 719 52. Yamamoto, T., R. M. Lynch, R. Gautam, R. Matus-Nicodemos, S. D. Schmidt, K. L. Boswell, S.  
720 Darko, P. Wong, Z. Sheng, C. Petrovas, A. B. McDermott, R. A. Seder, B. F. Keele, L. Shapiro, D.  
721 C. Douek, Y. Nishimura, J. R. Mascola, M. A. Martin, and R. A. Koup. 2015. Quality and  
722 quantity of TFH cells are critical for broad antibody development in SHIVAD8 infection.  
723 *Science translational medicine* 7: 298ra120.
- 724 53. Havenar-Daughton, C., M. Lindqvist, A. Heit, J. E. Wu, S. M. Reiss, K. Kendric, S. Belanger, S. P.  
725 Kasturi, E. Landais, R. S. Akondy, H. M. McGuire, M. Bothwell, P. A. Vagefi, E. Scully, I. P. C. P.  
726 Investigators, G. D. Tomaras, M. M. Davis, P. Pognard, R. Ahmed, B. D. Walker, B. Pulendran,  
727 M. J. McElrath, D. E. Kaufmann, and S. Crotty. 2016. CXCL13 is a plasma biomarker of  
728 germinal center activity. *Proceedings of the National Academy of Sciences of the United*  
729 *States of America* 113: 2702-2707.
- 730 54. Havenar-Daughton, C., D. G. Carnathan, A. Torrents de la Pena, M. Pauthner, B. Briney, S. M.  
731 Reiss, J. S. Wood, K. Kaushik, M. J. van Gils, S. L. Rosales, P. van der Woude, M. Locci, K. M.  
732 Le, S. W. de Taeye, D. Sok, A. U. Mohammed, J. Huang, S. Gumber, A. Garcia, S. P. Kasturi, B.  
733 Pulendran, J. P. Moore, R. Ahmed, G. Seumo, D. R. Burton, R. W. Sanders, G. Silvestri, and S.  
734 Crotty. 2016. Direct Probing of Germinal Center Responses Reveals Immunological Features  
735 and Bottlenecks for Neutralizing Antibody Responses to HIV Env Trimer. *Cell reports* 17:  
736 2195-2209.
- 737 55. Buranapraditkun, S., F. Pissani, J. E. Teigler, B. T. Schultz, G. Alter, M. Marovich, M. L. Robb,  
738 M. A. Eller, J. Martin, S. Deeks, N. L. Michael, and H. Streeck. 2017. Preservation of Peripheral  
739 T Follicular Helper Cell Function in HIV Controllers. *Journal of virology* 91.
- 740 56. Tomaras, G. D., N. L. Yates, P. Liu, L. Qin, G. G. Fouda, L. L. Chavez, A. C. Decamp, R. J. Parks,  
741 V. C. Ashley, J. T. Lucas, M. Cohen, J. Eron, C. B. Hicks, H. X. Liao, S. G. Self, G. Landucci, D. N.  
742 Forthal, K. J. Weinhold, B. F. Keele, B. H. Hahn, M. L. Greenberg, L. Morris, S. S. Karim, W. A.  
743 Blattner, D. C. Montefiori, G. M. Shaw, A. S. Perelson, and B. F. Haynes. 2008. Initial B-cell  
744 responses to transmitted human immunodeficiency virus type 1: virion-binding  
745 immunoglobulin M (IgM) and IgG antibodies followed by plasma anti-gp41 antibodies with  
746 ineffective control of initial viremia. *Journal of virology* 82: 12449-12463.

- 747 57. Trama, A. M., M. A. Moody, S. M. Alam, F. H. Jaeger, B. Lockwood, R. Parks, K. E. Lloyd, C.  
748 Stolarchuk, R. Scearce, A. Foulger, D. J. Marshall, J. F. Whitesides, T. L. Jeffries, Jr., K. Wiehe,  
749 L. Morris, B. Lambson, K. Soderberg, K. K. Hwang, G. D. Tomaras, N. Vandergrift, K. J. Jackson,  
750 K. M. Roskin, S. D. Boyd, T. B. Kepler, H. X. Liao, and B. F. Haynes. 2014. HIV-1 envelope gp41  
751 antibodies can originate from terminal ileum B cells that share cross-reactivity with  
752 commensal bacteria. *Cell host & microbe* 16: 215-226.
- 753 58. Williams, W. B., H. X. Liao, M. A. Moody, T. B. Kepler, S. M. Alam, F. Gao, K. Wiehe, A. M.  
754 Trama, K. Jones, R. Zhang, H. Song, D. J. Marshall, J. F. Whitesides, K. Sawatzki, A. Hua, P. Liu,  
755 M. Z. Tay, K. E. Seaton, X. Shen, A. Foulger, K. E. Lloyd, R. Parks, J. Pollara, G. Ferrari, J. S. Yu,  
756 N. Vandergrift, D. C. Montefiori, M. E. Sobieszczyk, S. Hammer, S. Karuna, P. Gilbert, D.  
757 Grove, N. Grunenber, M. J. McElrath, J. R. Mascola, R. A. Koup, L. Corey, G. J. Nabel, C.  
758 Morgan, G. Churchyard, J. Maenza, M. Keefer, B. S. Graham, L. R. Baden, G. D. Tomaras, and  
759 B. F. Haynes. 2015. HIV-1 VACCINES. Diversion of HIV-1 vaccine-induced immunity by gp41-  
760 microbiota cross-reactive antibodies. *Science* 349: aab1253.
- 761 59. Sender, R., S. Fuchs, and R. Milo. 2016. Revised Estimates for the Number of Human and  
762 Bacteria Cells in the Body. *PLoS biology* 14: e1002533.
- 763 60. Mouquet, H., and M. C. Nussenzweig. 2012. Polyreactive antibodies in adaptive immune  
764 responses to viruses. *Cellular and molecular life sciences : CMLS* 69: 1435-1445.
- 765 61. Haynes, B. F., J. Fleming, E. W. St Clair, H. Katinger, G. Stiegler, R. Kunert, J. Robinson, R. M.  
766 Scearce, K. Plonk, H. F. Staats, T. L. Ortel, H. X. Liao, and S. M. Alam. 2005. Cardioplipin  
767 polyspecific autoreactivity in two broadly neutralizing HIV-1 antibodies. *Science* 308: 1906-  
768 1908.

769

770 **FIGURE LEGENDS**

771 **Figure 1. Early treatment of HIV-1-infected patients preserves the resting memory B-**  
772 **cells in the gut.**

773 (A) Flow cytometry was used to assess the total number and frequency of CD19<sup>+</sup> cells from  
774 patients given combination antiretroviral therapy (cART) either early after transmission (e-  
775 ART, black squares) or later on, during the chronic phase of the disease (l-ART, grey squares)  
776 and from healthy HIV-1-negative controls (white squares). (B) Gut B-cell subpopulations  
777 identified by flow cytometry. (C) Frequencies of mature naive B cells (MN, CD21<sup>+</sup> CD27<sup>-</sup>),  
778 resting memory B cells (RM, CD21<sup>+</sup> CD27<sup>+</sup>), activated memory B cells (AM, CD21<sup>-</sup> CD27<sup>+</sup>),  
779 and tissue-like memory B cells (TLM, CD21<sup>-</sup> CD27<sup>-</sup>) within the CD19<sup>+</sup> CD38<sup>low</sup> CD10<sup>-</sup>  
780 mature B-cell population. Horizontal lines depict mean values. Kruskal-Wallis test: ns,  
781 nonsignificant; \*  $P < 0.05$  and \*\* $P < 0.01$

782

783 **Figure 2. Early treatment of HIV-1-infected patients preserves the IgA / IgG-secreting**  
784 **cell ratio in the gut.**

785 (A) Frequency of antibody-secreting cells (ASCs), i.e., plasmablasts/plasma cells, among total  
786 CD19<sup>+</sup> CD10<sup>-</sup> mature cells in the e-ART (black squares) and l-ART (grey squares) HIV-1-  
787 infected patients and healthy controls (white squares), evaluated by flow cytometry. (B)  
788 Concentrations of total IgGs and IgAs released spontaneously in the supernatant by mucosal  
789 ASCs from patients after 6 days of culture, evaluated by ELISA. Horizontal lines depict mean  
790 values. Kruskal-Wallis test: ns, nonsignificant; \*  $P < 0.05$  and \*\* $P < 0.01$ . (C) B-cell clonality  
791 analysis of total mucosal B cells in early- and late-treated patients with HIV-1 infection. Total  
792 mucosal B-cell repertoire in the early-treated (e-ART, black lines) and late-treated (l-ART,  
793 grey lines) patients, studied by PCR. DNA extracted from frozen sections of rectal mucosa  
794 from HIV-1-infected patients was subjected to CDRH3 PCR amplification using VH- and JH-

795 primers, as detailed in Methods. Representative normal CDR3-size distribution of the  
796 polyclonal profiles in the e-ART and l-ART groups is shown. **(D)** Clonality profile of the  
797 mucosal B-cell repertoire from 3 e-ART and 1 l-ART patients showing small expanded clonal  
798 populations (arrows). **(E)** Dot plot comparing the mucosal B-cell repertoires of e-ART (n=12)  
799 and l-ART patients (n=12). The number of B-cell expansions in each group is shown in the  
800 top panel, where each symbol represents a donor. The frequency of patients harboring B-cell  
801 expansions is given in the pie charts (bottom panel); the number in the middle of each chart is  
802 the number of patients. The two-sided nonparametric Mann-Whitney U test.

803

804 **Figure 3. Follicular helper T cells ( $T_{FH}$ ) are expanded in the gut of early-treated HIV-1-**  
805 **infected patients.**

806 **(A)** Gating strategy of mucosal  $T_{FH}$  cells **(B)** Frequencies of mucosal  $T_{FH}$  cells ( $CXCR5^+$   
807  $PD1^{high}$   $BCL6^+$ ) within the  $CD3^+CD4^+$  T-cell population in the HIV-1-infected patients and  
808 healthy controls. Horizontal lines depict mean values. Kruskal-Wallis test: ns, nonsignificant;  
809  $*P<0.05$ ;  $**** P<0.0001$ . **(C)** Correlation between the frequencies of  $T_{FH}$  cells and RM B  
810 cells in the gut, assessed using Spearman's rank order test. **(D)** Blood circulating- $T_{FH}$ -cell  
811 subpopulations identified by flow cytometry. **(E)** Frequency of total pre- $T_{FH}$  cells  
812 ( $CD3^+CD4^+CXCR5^+CCR7^-$ ) and frequencies of  $CXCR3^+CCR6^-$  (c- $T_{FH}1$ ),  $CXCR3^-CCR6^-$  (c-  
813  $T_{FH}2$ ), and  $CXCR3^-CCR6^+$  (c- $T_{FH}17$ ) within the  $CD3^+CD4^+CXCR5^+CCR7^-$  T-cell  
814 population. Horizontal lines depict mean values. Kruskal-Wallis test: ns, nonsignificant.

815

816 **Figure 4. Lymphoid structures in the gut of early-treated patients are permissive for the**  
817 **maintenance of  $T_{FH}$  cells.**

818 **(A)** Representative immunohistological stains for Pax5 (top panels) and PD-L1 (bottom  
819 panels) in rectal biopsies from patients given e-ART (n=6, left panels) or l-ART (n=6, right

820 panels). (B) The table lists the biopsies with and without PD-L1 expression (PD-L1<sup>+</sup> and PD-  
821 L1<sup>-</sup>, respectively). The asterisk indicates absence of co-localization between PD-L1 and Pax5  
822 staining.

823

824 **Figure 5. HIV-1 Env gp140-reactive B cells are expanded in the gut of early-treated**  
825 **HIV-1-infected patients and correlate with the frequency of gut-resident T<sub>FH</sub> cells.**

826 (A) Representative dot plots of gp140-reactive mucosal B cells from healthy HIV-1-negative  
827 controls (HIV<sup>-</sup>) and HIV-1-infected patients (HIV<sup>+</sup>). (B) and (C) Total mucosal HIV-1-  
828 gp140-reactive CD19<sup>+</sup> cells: frequencies (B) and (C) distribution among the different B-cell  
829 compartments. (D) B-cell receptor (BCR) isotypes expressed by the gp140-reactive resting  
830 memory (RM) B cells in the e-ART and l-ART groups, compared using the two-sided  
831 nonparametric Mann-Whitney U test: \**P*<0.05. (E) Correlation between the frequencies of  
832 mucosal T<sub>FH</sub> cells and gp140-reactive CD19<sup>+</sup> cells in the gut, assessed using Spearman's rank  
833 order test. (F) Reactivity against immobilized gp140 of total IgG (2 μg/mL) released by  
834 mucosal ASCs, either spontaneously (without stimulation) or following *in vitro* differentiation  
835 (IL-4, IL-21, and anti-CD40). The two-sided nonparametric Mann-Whitney U test was used:  
836 ns, nonsignificant and \**P*<0.05.

837

838 **Figure 6. Higher frequency of HIV-1-specific-IL21 secreting T cells in the blood of early-**  
839 **treated patients.**

840 (A) and (B) The graphs depict the concentrations of IL-21 and IFN-γ released in the  
841 supernatant by total peripheral blood mononuclear cells (PBMCs, 5·10<sup>5</sup> cells per well) from e-  
842 ART and l-ART patients (A) after stimulation with *Staphylococcus aureus* endotoxin B  
843 superantigen (SEB, 50 ng/mL) or (B) a pool of peptides derived from the HIV-1 Gag  
844 polyprotein and HIV-1 Env glycoprotein gp160 (HIV-1 antigens, all 1 μg/mL), for 6 days.

845 Horizontal lines depict median values. Two-sided nonparametric Mann-Whitney U test: ns,  
846 nonsignificant and  $*P<0.05$ .

847

848 **Supplemental Figure 1. Early treatment of HIV-1-infected patients preserves resting**  
849 **memory B-cells in blood.** Frequencies of mature naive B cells (MN, CD21+ CD27-), resting  
850 memory B cells (RM, CD21+ CD27+), activated memory B cells (AM, CD21-CD27+), and  
851 tissue-like memory B cells (TLM, CD21- CD27-) among CD19+ CD38<sup>low</sup> CD10- mature B  
852 cells in the blood from early-treated patients (e-ART, blue squares) and late-treated patients  
853 (l-ART, red squares) and from healthy HIV-negative controls (HIV-, white squares).

854

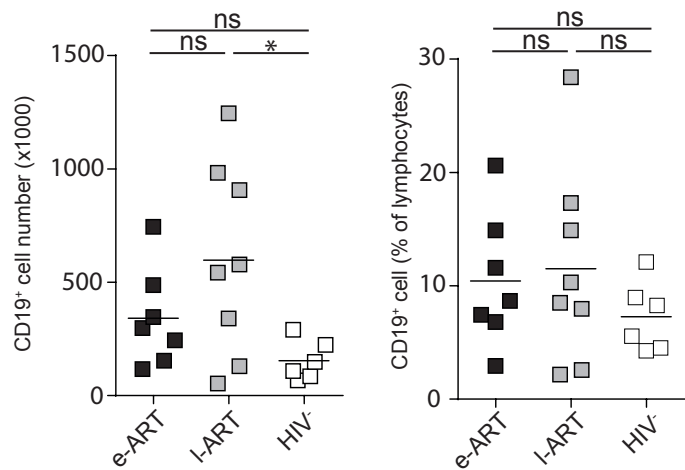
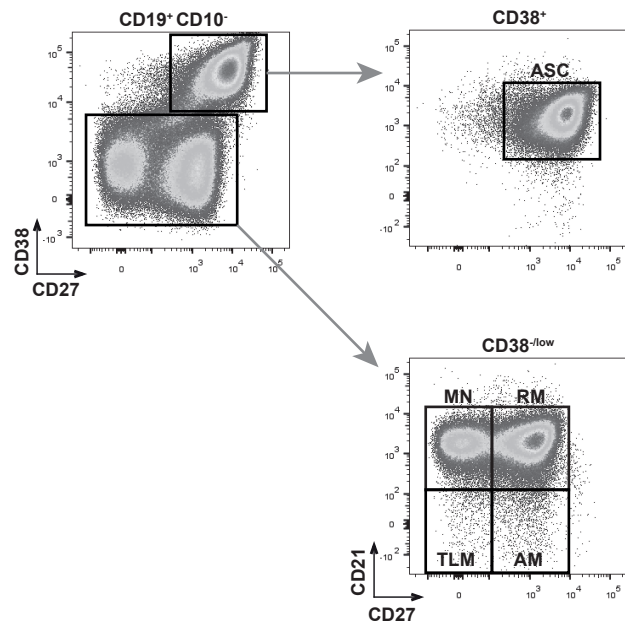
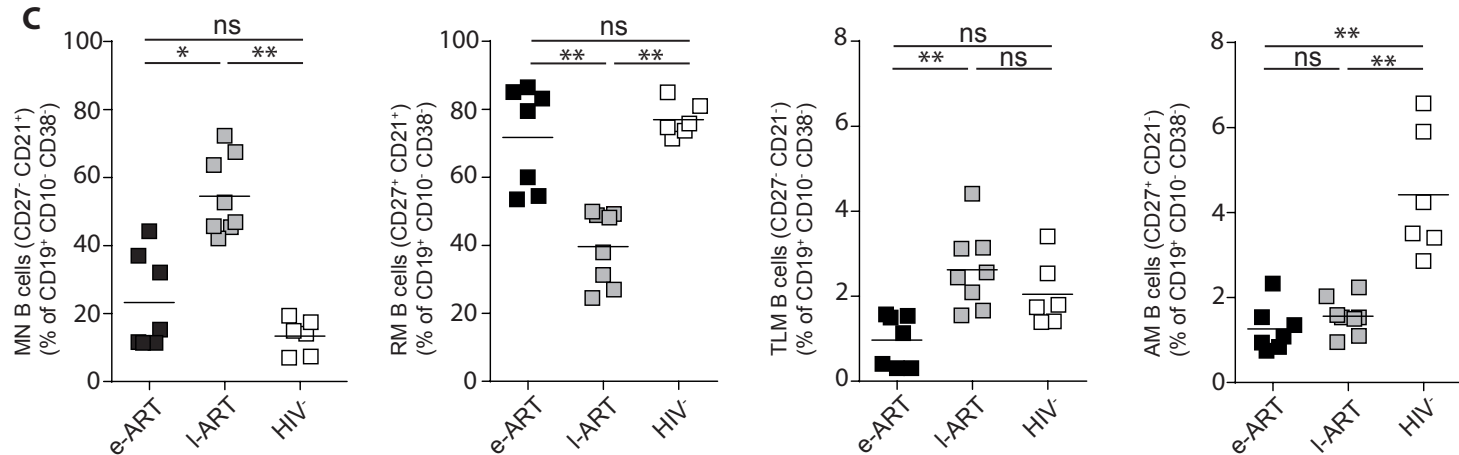
855 **Supplemental Figure 2. mRNA factors important for the germinal center's functions are**  
856 **higher in the gut of early-treated HIV-1-infected patients. (A)** IL-6-, IL-27p28-, IL-27  
857 EBI-3-, and IL-12A mRNA expressions in rectal biopsies of HIV-1-infected patients,  
858 quantified by qPCR. The histograms depict mean $\pm$  SEM. The two-sided nonparametric Mann-  
859 Whitney U test was used: ns, non significant;  $*P<0.05$  **(B)** AICDA mRNA transcripts in  
860 rectal biopsies from the patients, quantified by qPCR. Histograms depict mean values  $\pm$  SEM.  
861 Kruskal-Wallis test: ns, non significant and  $**P<0.01$ .

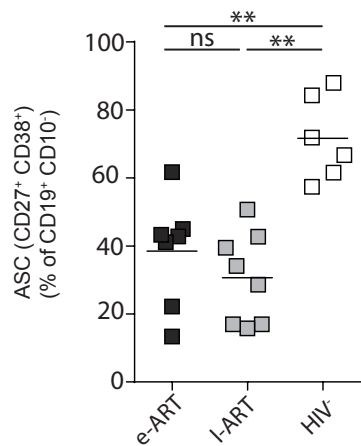
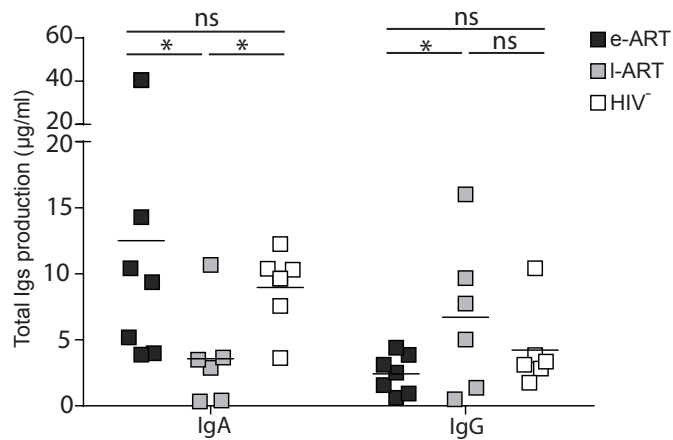
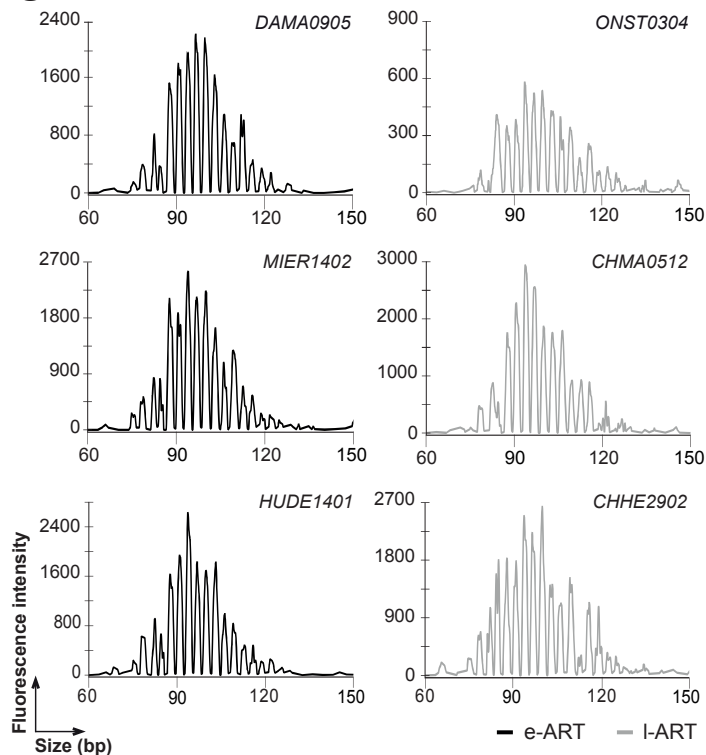
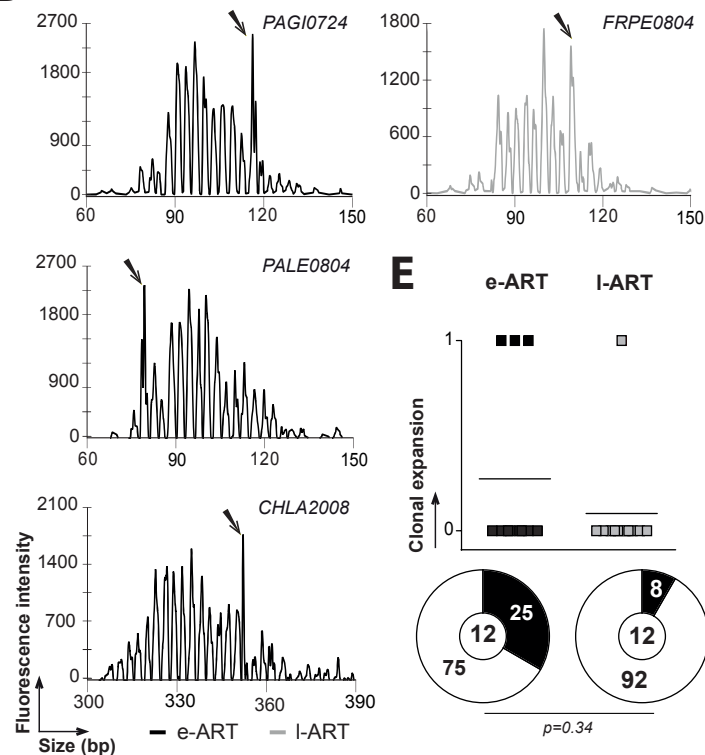
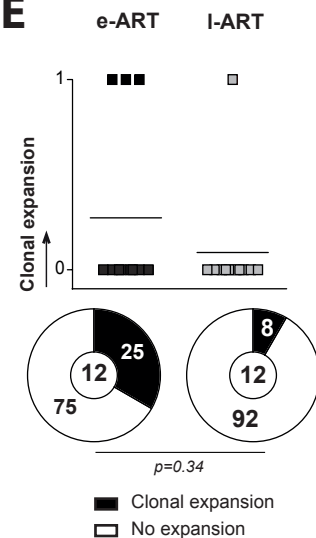
862

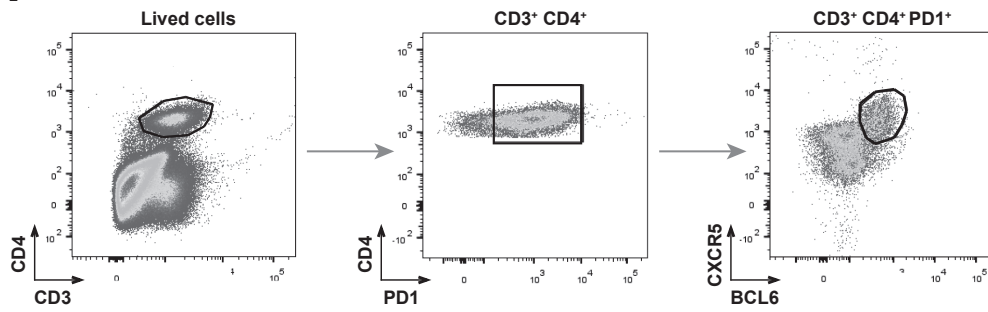
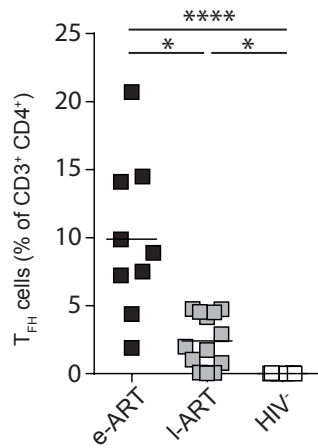
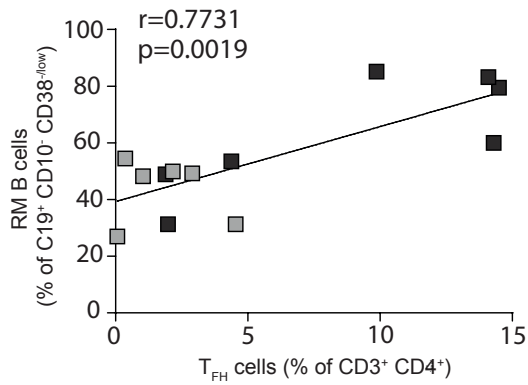
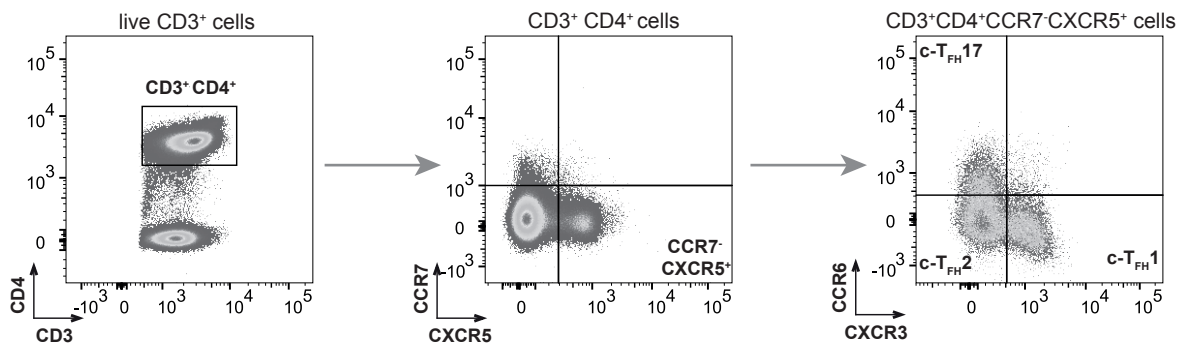
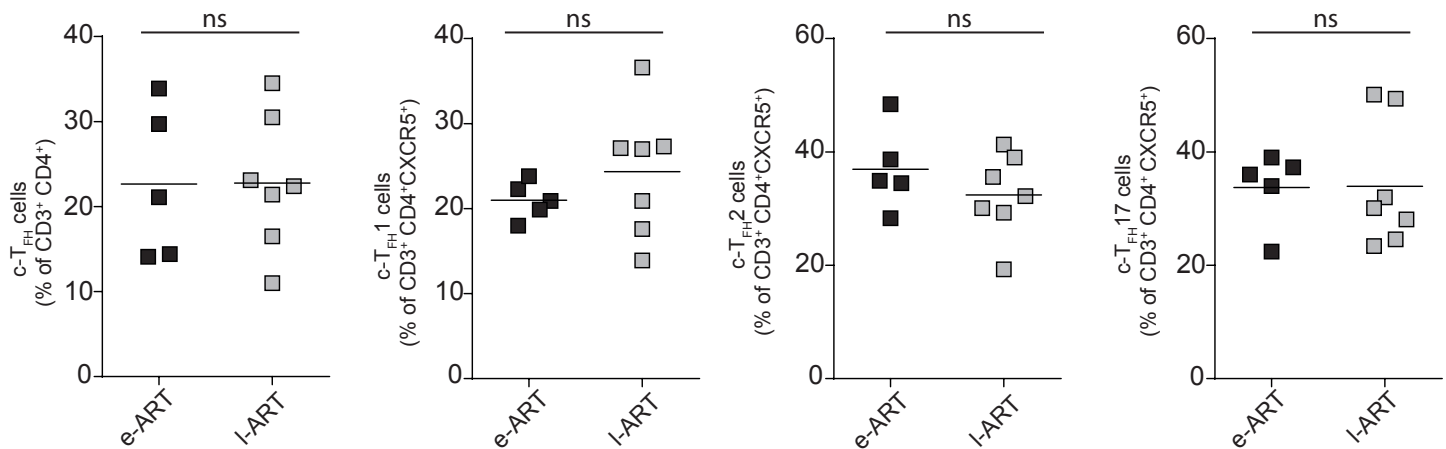
863 **Supplemental Figure 3. The frequency of gp140-reactive B cells is higher in the blood of**  
864 **early-treated HIV-1-infected patients.**

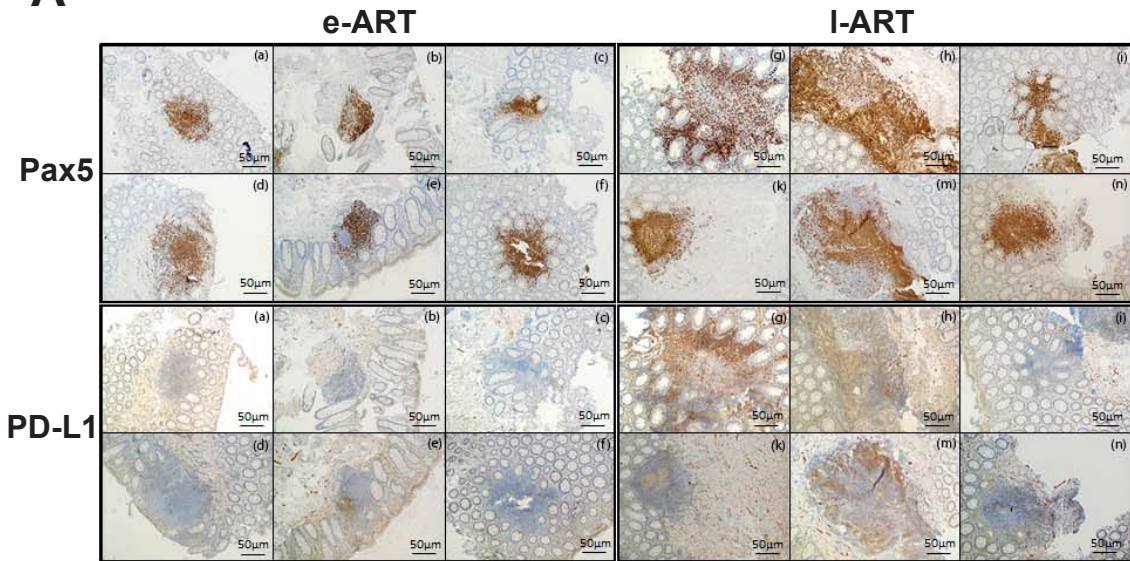
865 Frequencies of total gp140-reactive CD19+ cells in the blood and gut of e-ART and l-ART  
866 patients. Two-sided nonparametric Mann- Whitney U test:  $*P<0.05$ .

867

**A****B****C**

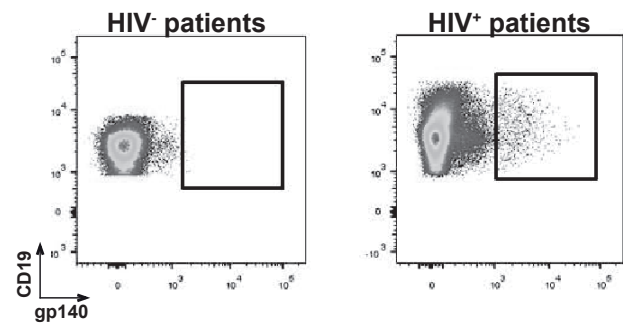
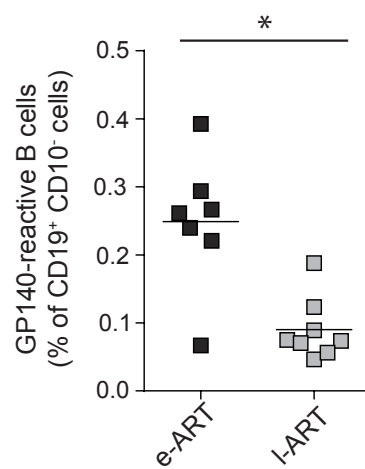
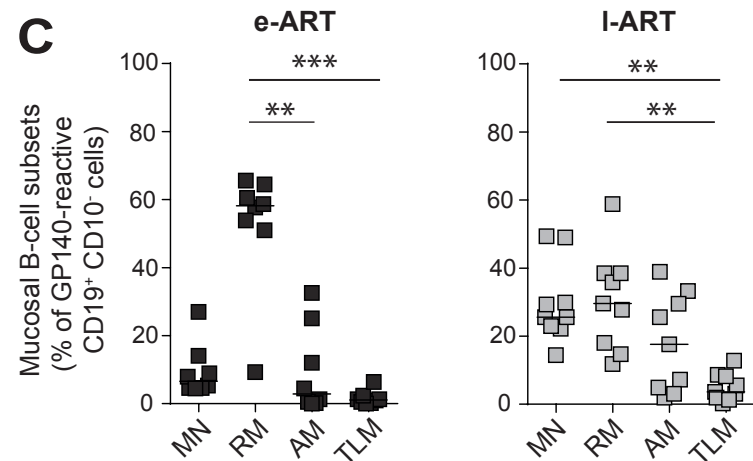
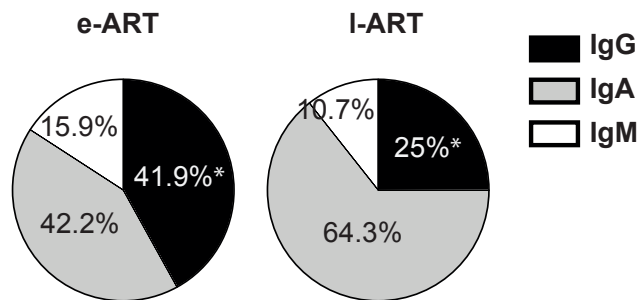
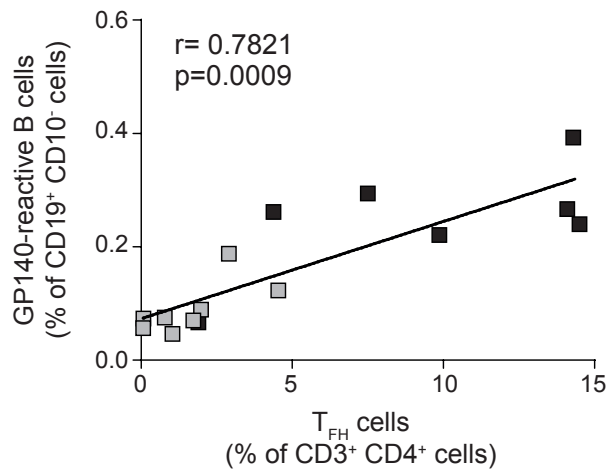
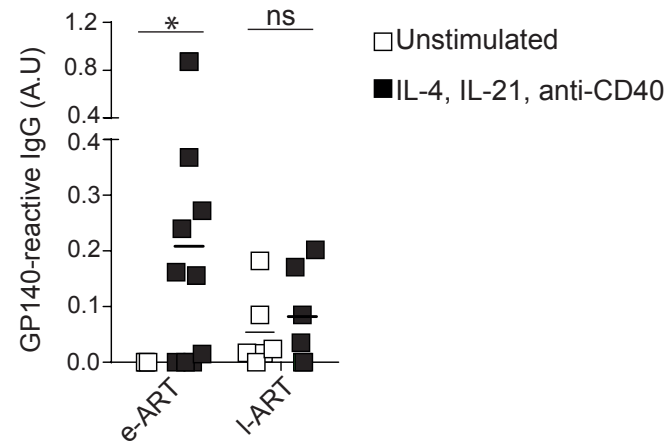
**A****B****C****D****E**

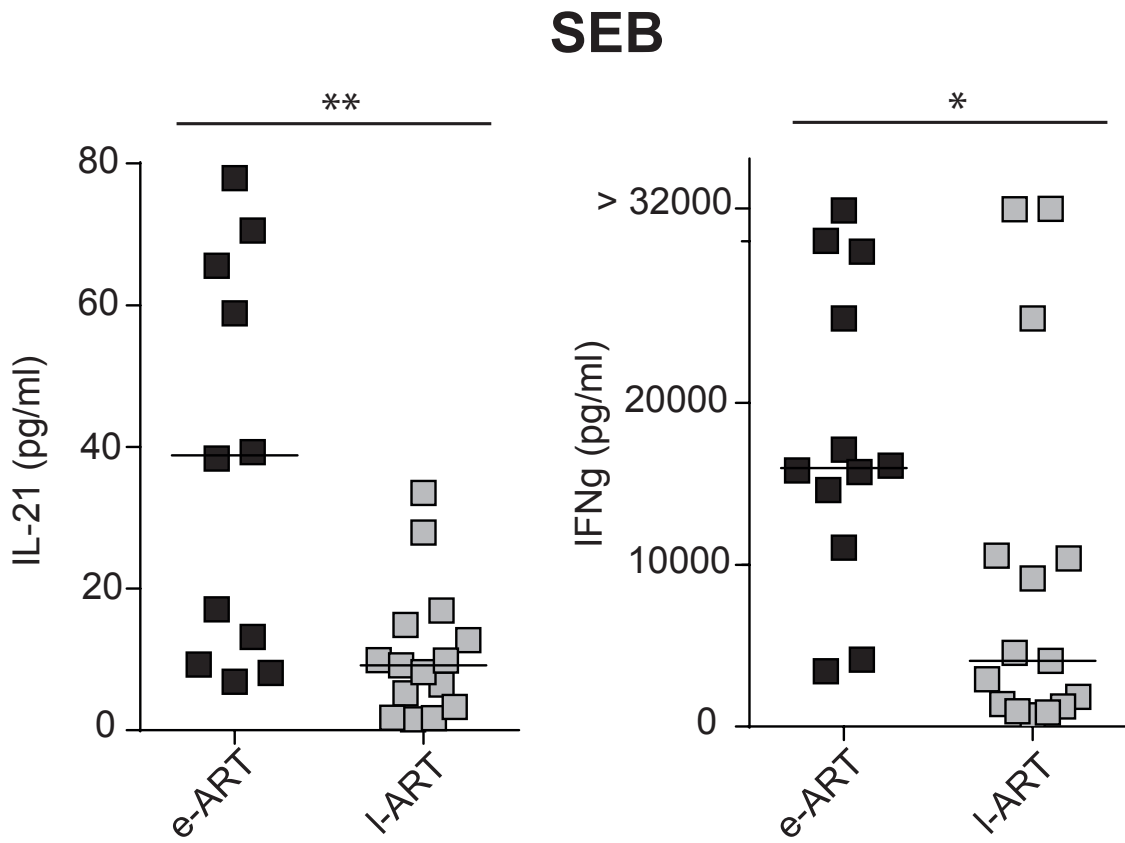
**A****B****C****D****E**

**A****B**

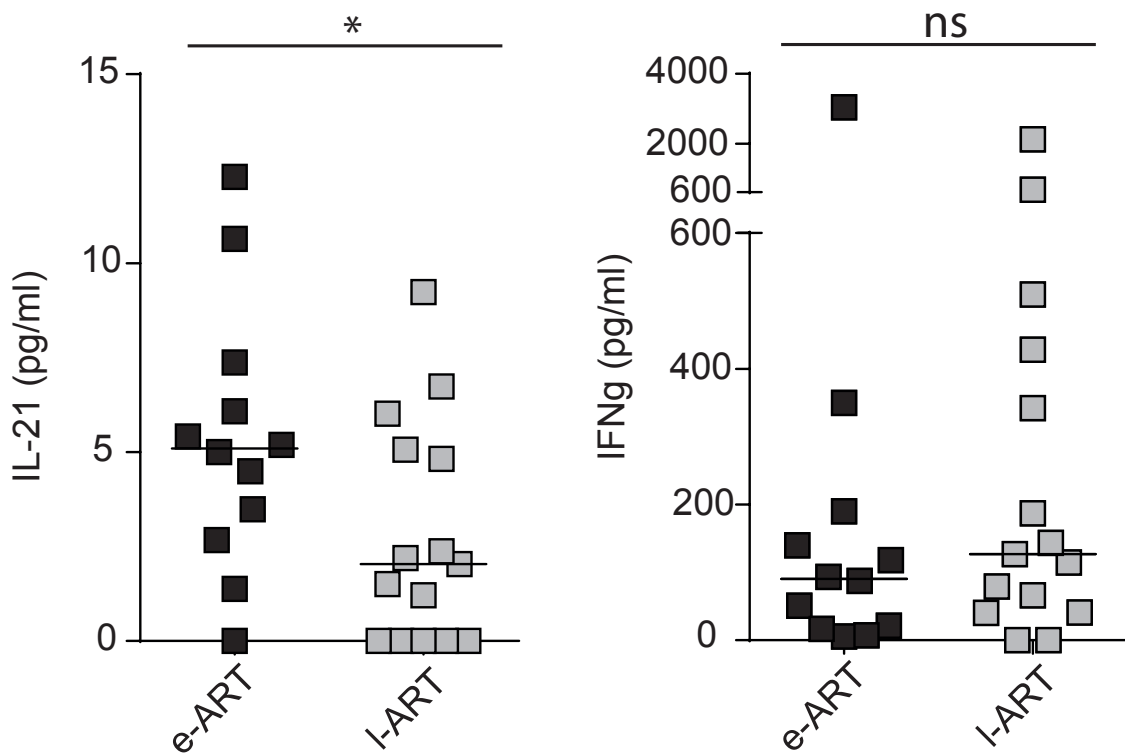
	Early cART	Late cART
	n=6	n=6
PD-L1 <sup>-</sup>	(a) (b) (c) (d) (f)	(i)
PD-L1 <sup>+</sup>	(e)*	(g) (h) (k) (m)* (n)*

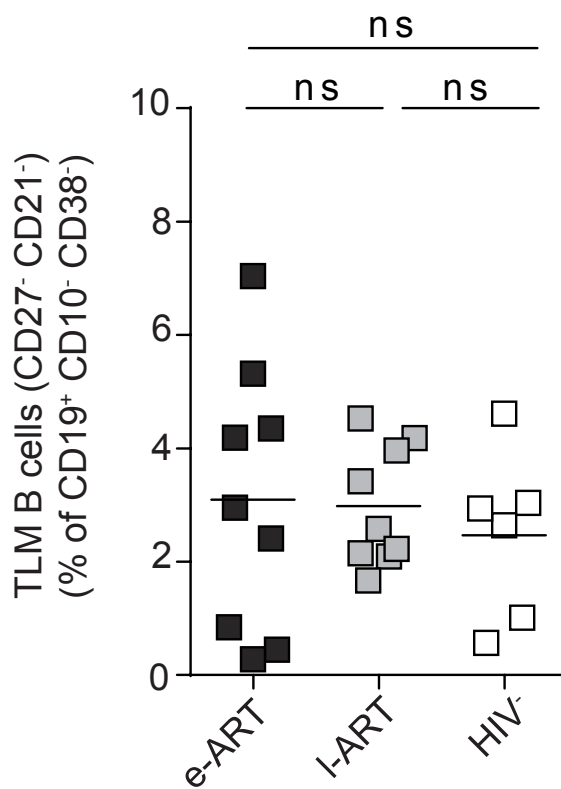
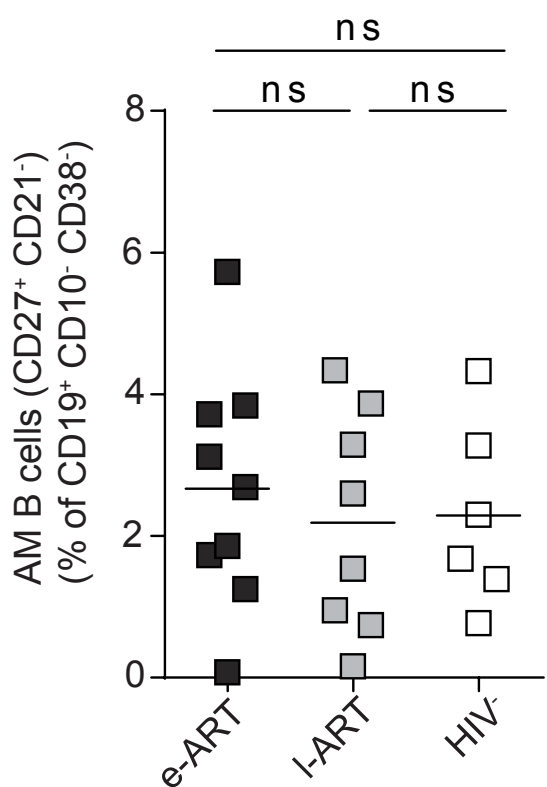
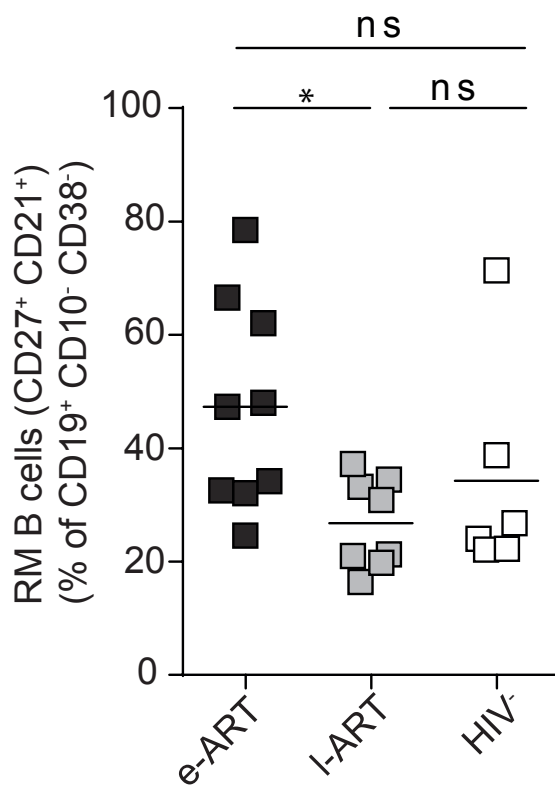
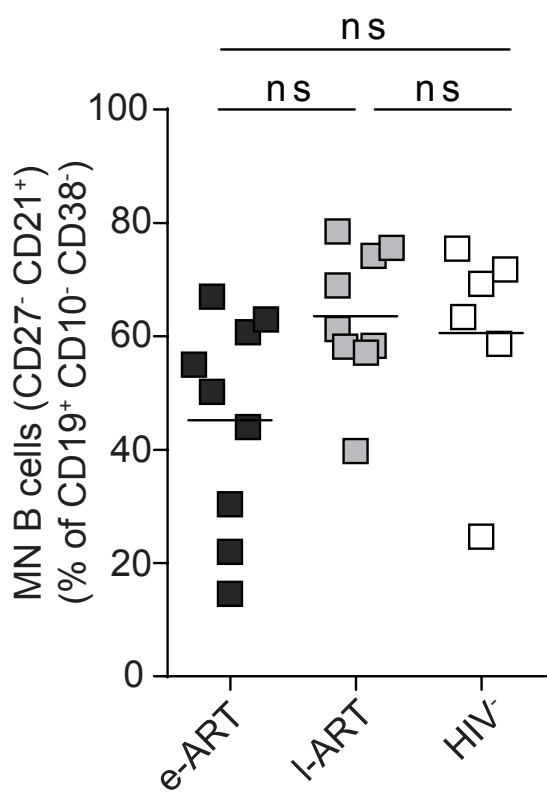
\*: PD-L1 staining not colocalized with Pax5 staining

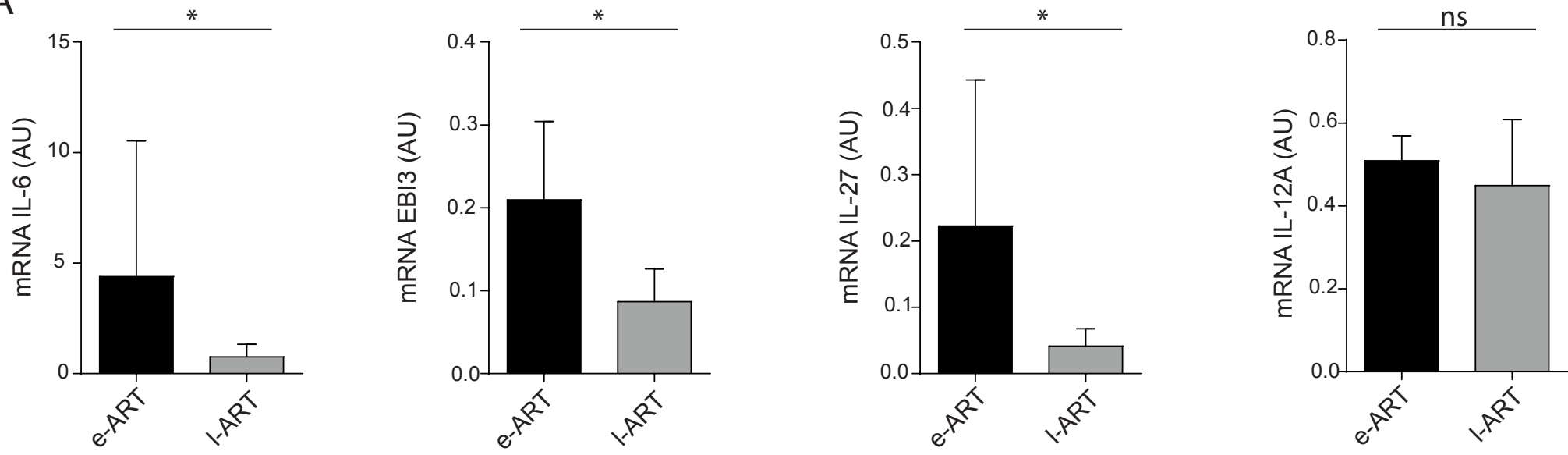
**A****B****C****D****E****F**

**A****B**

### HIV-1 (gag+env peptides)





**A****B**